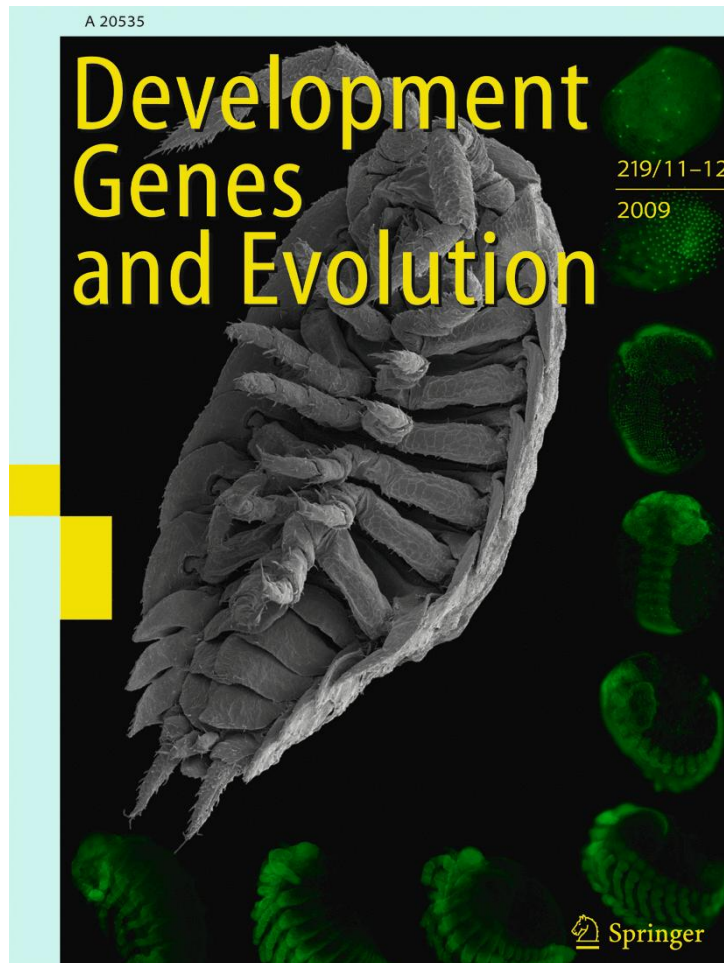


ISSN 0949-944X, Volume 219, Combined 11-12



**This article was published in the above mentioned Springer issue.
The material, including all portions thereof, is protected by copyright;
all rights are held exclusively by Springer Science + Business Media.**

**The material is for personal use only;
commercial use is not permitted.**

**Unauthorized reproduction, transfer and/or use
may be a violation of criminal as well as civil law.**

The embryonic development of the malacostracan crustacean *Porcellio scaber* (Isopoda, Oniscidea)

Carsten Wolff

Received: 22 September 2009 / Accepted: 31 December 2009 / Published online: 29 January 2010
© Springer-Verlag 2010

Abstract To examine the evolution of development and put it into a phylogenetic context, it is important to have, in addition to a model organism like *Drosophila*, more insights into the huge diversity of arthropod morphologies. In recent years, the malacostracan crustacean *Porcellio scaber* Latreille, 1804 has become a popular animal for studies in evolutionary and developmental biology, but a detailed and complete description of its embryonic development is still lacking. Therefore, the embryonic development of the woodlouse *P. scaber* is described in a series of discrete stages easily identified by examination of living animals and the widely used technique of nuclei staining on fixed specimens. It starts with the first cleavage of the zygote and ends with a hatched manca that eventually leaves the mother's brood pouch. Classical methods like normal light microscopy, scanning electron microscopy and fluorescence microscopy are used, in addition to confocal LCM and computer-aided 3D reconstruction in order to visualise important processes during ontogeny. The purpose of these studies is to offer an easy way to define the different degrees of development for future comparative analyses of embryonic development amongst crustaceans in particular, as well as between different arthropod groups. In addition, several aspects of *Porcellio* embryonic development, such as the mouth formation, limb differentiations

and modifications or the formation of the digestive tract, make this species particularly interesting for future studies in evolutionary and developmental biology.

Keywords Arthropods · Isopoda · Embryogenesis · Evolution · Direct development · Crustacea

Introduction

Evolutionary developmental biology thrives on comparisons of developmental processes of different animals and plants in an attempt to infer the ancestral relationship between organisms. The main focus is to examine the evolution of embryonic development: how modifications of development and developmental processes lead to the production of novel features. Crustaceans are an enormously successful group of arthropods. One of the most speciose groups within Crustacea is the Isopoda. As a malacostracan crustacean, *Porcellio scaber* is one of a few representative organisms which are suitable for comparative research in evolutionary and developmental biology. *Porcellio* is distributed worldwide and is already established as a favoured standard organism in ecological and toxicological studies (e.g. [Drobne 1997](#); [Zidar et al. 2009](#)). *Porcellio* displays a direct development, with the eggs developing inside a ventral brood pouch, where they hatch as mancas. The ventral brood pouch (so-called marsupium) functions as a micro-aquarium that allows embryonic development to occur without an external water source ([Hoese and Janssen 1989](#)). Because of its easy maintenance and the fact that eggs are available all year around, this isopod was a favourable choice for diverse developmental studies. Details of gastrulation and early germ band formation were investigated via 4D microscopy by [Hejnol et al. \(2006\)](#).

Communicated by S. Roth

Electronic supplementary material The online version of this article (doi:10.1007/s00427-010-0316-6) contains supplementary material, which is available to authorized users.

C. Wolff (✉)
Institut für Biologie, Humboldt-Universität zu Berlin,
Philippstr. 13,
10115 Berlin, Germany
e-mail: carsten.wolff@rz.hu-berlin.de

Shortly after gastrulation, a complex invariant cell division pattern of the post-naupliar germ band is formed by ectotoloblasts. The generation of genealogical units of the trunk ectoderm in an anterior direction is typical for malacostracan development (e.g. Dohle and Scholtz 1988, 1997; Scholtz and Dohle 1996; Dohle et al. 2004). These genealogical units subsequently undergo stereotyped cell division patterns that allow us to trace the fate of individual cells. Thus, a very detailed analysis of the gene expression patterns of *engrailed* and *Distal-less* was undertaken up to the early limb bud formation (Hejnal and Scholtz 2004). Extensive studies of gene expression patterns (Abzhanov and Kaufmann 1999a, b, 2000a, b, 2004; Brena et al. 2005) have been made as well as developmental studies on the nervous (Whittington et al. 1993), digestive (Strus et al. 2008) and muscular systems (Kreissl et al. 2008). However, detailed descriptive staging information covering the complete course of embryogenesis in isopods is largely lacking.

Although some of these authors developed a staging system for their research, it lacks a complete sequence of the embryonic development. Whittington et al. (1993) proposed the most detailed staging system based on the embryonic age. But unfortunately, this method seems to be inappropriate for *Porcellio* because there are considerable differences in the developmental rate amongst the eggs of different broods.

To keep up with detailed staging information which is available for some other arthropods like the insect *Drosophila melanogaster* (Campos-Ortega and Hartenstein, 1997; Hartenstein 1993) or the amphipod crustacean *Parhyale hawaiiensis* (Browne et al. 2005), a detailed description of the morphology of the developmental stages, through which the embryo passes, is indispensable. Therefore, the embryonic development of the isopod *P. scaber* is described by using scanning electron microscopy (SEM) and fluorescence staining. The result is a series of discrete stages easily identified by examination of living animals and the use of simple fluorescence markers on fixed specimens. In addition to its usefulness as a basis for future studies, several aspects of the embryonic development make this species particularly interesting for future studies.

Material and methods

Individuals of *P. scaber* were collected in and around Berlin. Populations of the species were cultured in our laboratory. The eggs, embryos and manca were isolated from the ventral brood pouch (marsupium) of the egg-bearing females using a glass pipette. *P. scaber* undergoes direct development and, therefore, passes through all the developmental stages within the egg membranes. Prior to fixation, the egg membranes were carefully removed under a dissecting microscope using insect pins and tweezers.

For SEM, the embryos were fixed in Bouin's fluid (75% saturated aqueous picric acid solution, 20% saturated formaldehyde, 5% glacial acetic acid) between 10 and 60 min, dehydrated in a graded ethyl alcohol series and critical point dried with a CPD BALTEC 030 following standard procedures. The mounted specimens were sputtered with gold using a SCD BALTEC 005, and a Leo 1450VP was used to take SEM photographs.

The material for nuclear fluorescent dye staining was fixed by boiling in phosphate-buffered saline (PBS) for several minutes (<10 min), then washed with PBS and post-fixed for several hours in 4% formaldehyde (in PBS). The dye was nucleic-acid-specific Sytox Green (Molecular Probes). In addition to staining nuclei, it allows the visualisation of the cytoplasm of stained cells and thus the cell shape. Preserved specimens were washed in Tris buffer (TBS) several times, transferred to Sytox solution in TBS (1:1,000) and incubated for 3 h. Embryos were then washed again in TBS and mounted on microscopic slides in anti-bleaching medium (DABCO-Glycerol). Samples were analysed under fluorescence and light microscope (Zeiss Axioskop2, Zeiss Lumar) and a laser scanning microscope (Leica SP2). The laser-scanned image stacks were processed with the 3D reconstruction software Imaris. The computer-aided three-dimensional reconstructions allow us to not only see the embryos in total but also to investigate cell layers in different depths of the embryo.

Results

Whilst investigating the development of *P. scaber*, considerable differences in the developmental rate amongst the eggs of different broods and even within single broods were found, and the most common way to make a staging by age (as recommended by Whittington et al. 1993) seemed inappropriate. Beginning with the fertilised zygotes until the release of manca larvae, the embryonic development of *P. scaber* can be split into 20 distinct stages. Each stage is characterised by developmental events or important features in morphogenesis and organogenesis. An isopod body is typically divided into three major tagmata. The cephalothorax bears two pairs of antennae, a mandible, a first and a second maxilla and the first thoracopod (called maxilliped). The pereon bears seven pairs of uniramous thoracopods (pereopods). The pleon bears six biramous limbs of which some are specialised into branchial structures. The endopods of the third to fifth pleopods are differentiated into gills (e.g. Schram 1986; Gruner 1965, 1993). For life on land, terrestrial isopods evolved additional features like a cuticular water transport system to collect water from the environment (Hoese 1981) or pseudotracheae (modified exopods of the first and second pleopod) to get oxygen

directly from the air (Hoese 1983; Schmidt and Wägele 2001). The last pleomere is fused to the telson, forming a so-called pleotelson, and bears the uropods (sixth pleopods) which have a tail-like character.

Zygote

Fertilised eggs of *P. scaber* are about 400 to 600 μm in diameter. Because of the compact package of up to 40 eggs in the female's ventral brood pouch (marsupium) the shape of the eggs can vary from angular to oval (Fig. 1). Under the light microscope, the nucleus appears as a more condensed region in the egg centre (Fig. 1a). The surrounding transparent yolk consists of globular yolk granules and can show a colour range from greenish to yellowish to brownish but is consistent in a single offspring. The external egg envelope (chorion) loosely surrounds the egg whilst the internal layer (vitelline membrane) fits closer to the embryo (Fig. 1a, b).

Early cleavages

Eggs undergo superficial intralecithal cleavage; the nuclei divide within the evenly distributed yolk mass without

forming cell membranes. After the first division into the two-nuclei stage, the nuclei remain in the centre of the egg. Now, the appearance of the nucleonic region is denser than before (Fig. 1b). The division into the four-nuclei stage is synchronous, and the division directions are oblique to each other (Fig. 1c) so that the nuclei form a tetrahedron. At the beginning of the third synchronous division cycle, the nuclei start moving to the egg periphery. This process results in eight nuclei which lie more or less at the surface (Fig. 1d). The fourth division cycle is synchronous, and all 16 nuclei are evenly spread at the periphery of the centrolecithal egg (Fig. 1e). The fifth cleavage is the last synchronous cleavage (Fig. 1f). From now on, the nuclei lose their dense appearance and are not easily detectable under normal light microscope.

Germ disc

From the 32-nuclei stage onward, the divisions are no longer synchronous. Most of the nuclei migrate to one pole of the egg and form a circular cell aggregation of about 30 cells—the early germ disc (Fig. 2a). Nuclei staining (Sytox) show that at this time no cell membranes are formed, and the cleavage is still superficial. The ongoing growth of the

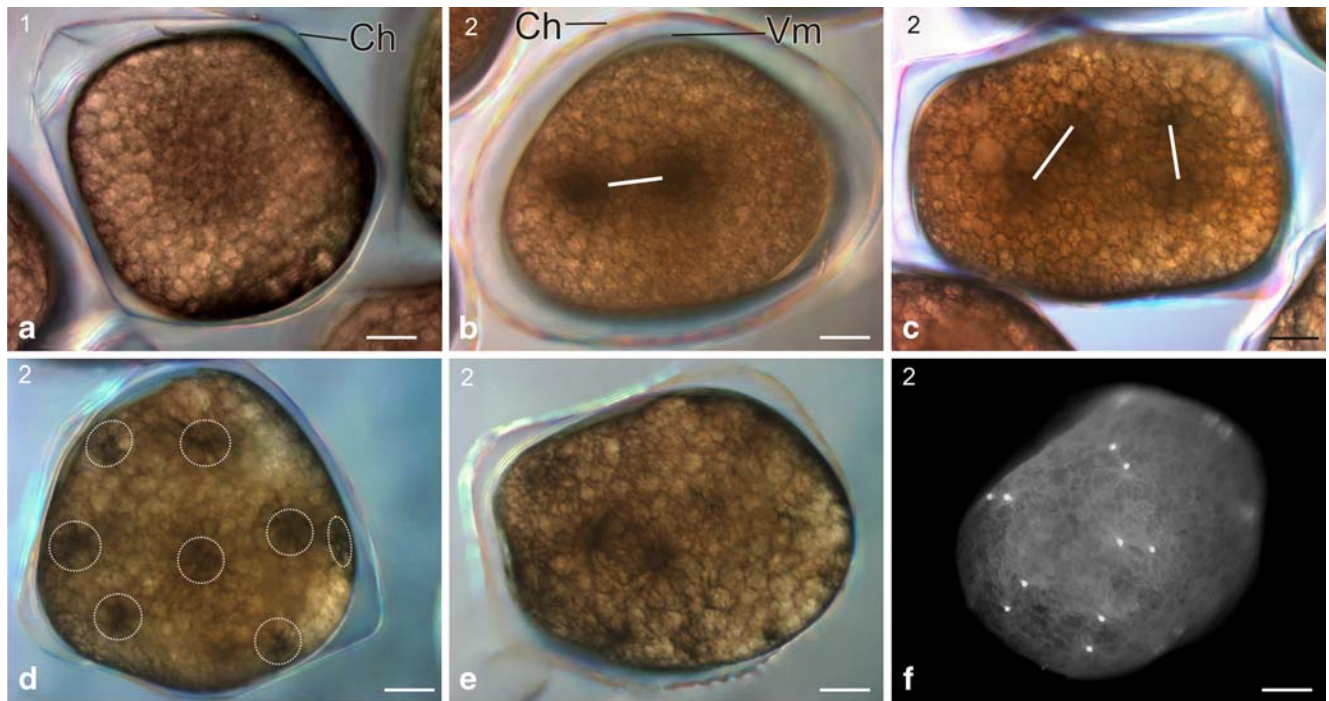


Fig. 1 Stages 1–2 of *P. scaber*. All scale bars show 100 μm . **a** Stage 1, zygote. The chorion (*Ch*) loosely encloses the egg which shows a central dense region—the nucleus. **b–f** Stage 2, first cleavages. **b** After the first cleavage, two nuclei in the centre of the granular yolk are visible as *dark spots*. The inner embryonic egg shell—the vitelline membrane (*Vm*)—fits closer to the egg. **c** Four-nuclei stage. The nuclei are still in the centre of the egg, and the division planes (*white*

bars) are oblique to each other. **d** Eight-nuclei stage. The nuclei (*white circles*) start to move towards the egg surface. **e** The fourth cleavage results in a 16-nuclei stage. The nuclei start to lose their dense appearance and become indiscernible under light microscopy. **f** Nuclei-stained egg during the fifth cleavage. The synchronous cleavage results into 32 nuclei

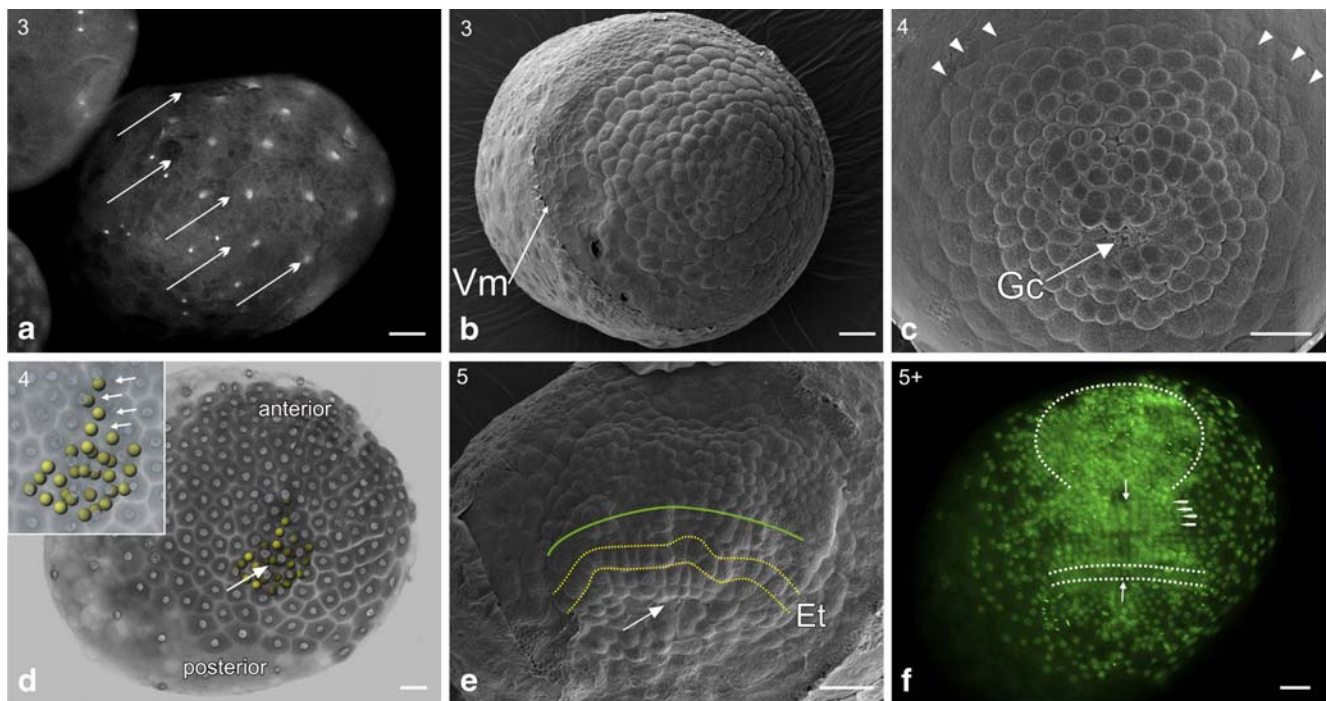


Fig. 2 Stages 3–5 of *P. scaber*. All scale bars show 50 μm . **a, b** Stage 3, germ disc formation. **a** Nuclei-stained egg after the sixth cleavage. The majority of the nuclei move to one egg pole and aggregate together (indicated by arrows). **b** Early germ disc with around 180 cells. The vitelline membrane (*Vm*) sticks to the egg and covers most of the extra-embryonic region. Note that the cells adjacent to the early germ disc still have no cell membranes. **c, d** Stage 4, gastrulation. **c** In the centre of the germ disc, the gastrulation centre (*Gc*) has formed where single cells move inwards. Lateral cells at the growing germ disc show membrane formation (arrowheads). **d** 3D reconstructed confocal image stack. The ectodermal cell layer is transparent, and the yellow spheres mark the mesendodermal cells (white arrow point to the blastopore). The small picture is a detail of the around 30 mesendodermal cells. Some cells started migrating anteriorly (little

arrows) and will give rise to the naupliar mesoderm. **e, f** Stage 5, ectoteloblasts. **e** Anterior to the blastopore (white arrow), a semi-circle of ectoteloblasts (*Et*) has formed (indicated by dotted yellow line). Anterior to the ectoteloblasts are cells which give rise to the segments of maxilla 1 and maxilla 2 (indicated by the green line). The cells anterior to the green line will give rise to the future naupliar region (head). **f** Nuclei-stained early germ band. The transverse cell row of ectoteloblasts (white lines) started the production of the post-naupliar ectoderm. Because of their high division activity, they show a less-intense expression. The cells of the segments of first and second maxilla (white arrowheads) are not the offspring of the ectoteloblasts but also arranged in a grid-like pattern. The medial midline is indicated by white arrows

germ disc is a combination of cell migration and the more rapid cell division that occurs amongst these cells compared to the cells which are not involved in the germ disc formation. When the cells aggregate together to form a germ disc, the formation of cell membranes starts. A distinct gradient that radiates outward from the germ disc region begins to become visible so that the germ disc surrounding tissue (so-called extra-embryonic tissue) still maintains a syncytial organisation (Fig. 2b).

Gastrulation

During further development, the germ disc consists of about 200 cells and covers 10–20% of the egg surface. Also, in the extra-embryonic region, cell membranes are formed (Fig. 2c). The germ disc is slightly bulged at the egg periphery, but because of its transparency, it is not detectable under light microscopy. Single cells located more or less in the centre of the germ disc start to migrate

inwards into the embryo and initiate the process of gastrulation (Fig. 2c). This region is marked by the formation of a blastopore. During the gastrulation process, the mesendodermal cell mass of about 30 cells shows a typical shape at several depth levels (Figs. 2c, d). A few cells start to migrate in an anterior direction and represent the naupliar mesendoderm (Fig. 2d). There are about four conspicuous cells in the deepest egg level which show a different, more granular expression of weak Sytox staining (Fig. 2d). It is likely that these cells are the first cells to separate from the blastoderm during the gastrulation process and probably give rise to the germ progenitor cells.

Ectoteloblasts

A late germ disc has a characteristic appearance. Two hemi-circles of cells surround the blastopore. The inner ring continues to generate cells which migrate inward during ongoing gastrulation. The outer ring consists of about ten

bigger cells which have a rectangular shape—the so-called ectoteloblasts (Fig. 2e). These cells are responsible for the generation of most of the post-naupliar ectoderm, beginning with the first thoracic segment. Anterior to the ectoteloblasts lie disordered cells which are the origin of the segments of the first and second maxilla (Fig. 2e). During further development, the cells which come from the ectoteloblasts have a very strict cell division pattern resulting in a grid-like arrangement (Fig. 2f). The population of cells anterior to the descendants of the ectoteloblasts reorganise themselves so that finally the same grid pattern appears (Fig. 2f). A medial unpaired and slightly sunken midline is visible along the complete post-naupliar ectoderm. Anterior to this, in the naupliar region, no pattern of cell arrangement is detectable (Figs. 2e, f). Underneath this naupliar area, the mesodermal and endodermal cells still remain as one common cell mass (mesendoderm).

Germ band

As the number of ectoteloblasts increases, this transverse row of cells (Fig. 3a) starts to produce cells which will form most of the post-naupliar ectoderm. Underneath the ectoteloblasts but shifted slightly anteriorly, eight mesoteloblasts—four on each body half—have similar characteristics and start to form the main parts of the post-naupliar mesoderm. In front of the forming grid pattern, the naupliar (head) region shows a bilobed appearance. No segmental differentiation is visible in this head region yet. Smaller, more subsided cells split the head primordia into a left and a right part and define a characteristic V-shaped medial naupliar region between the two sides (Figs. 3a, b).

Midgut primordium

The V-shaped character of the head region is more pronounced at this stage, and the nuclear staining shows distinct clusters with more cells. These clusters represent the optical lobes and the three naupliar segments antenna 1, antenna 2 and the mandibular segment (Fig. 3b). The mesendodermal cells underneath the naupliar ectoderm separate into more medial-lying naupliar mesodermal cells and the more lateral midgut primordium (endoderm). At this time, the midgut primordium is a group of cells which lies laterally adjacent to the segment of antenna 2 and mandible (Fig. 3b). The ectoteloblasts are highly active, producing cell rows (genealogical units) which are composed of an unpaired midline and paired lateral cells. These rows undergo two regular mitotic waves with longitudinally oriented spindle axes, thus resulting in a regular grid pattern in the post-naupliar region. The constant proliferation of new genealogical units leads to a developmental gradient from anterior to posterior.

Segment formation

The embryo is totally transparent and difficult to observe under light microscope (Fig. 3f). Labelling of the nuclei shows a much broader naupliar region with segmental clusters of antenna 1, antenna 2 and mandible. External segmental borders are not visible yet. In the narrow post-naupliar region, the ectoteloblasts are still active; the anterior genealogical units undergo differential cleavages, and the regular grid pattern disappears (Fig. 3c). The process of segmentation starts in the anterior embryonic region. Therefore, two adjacent genealogical units together form a morphological segment, which is split by the distinct midline (Fig. 3c).

Naupliar appendages

The first external morphogenetic differentiations are noticeable. Limb buds of the first and second antenna and the mandible start to develop (Fig. 3d). The midline is not visible any longer and intersegmental furrows appear between the segments of maxilla 2, maxilliped and in the anterior region of the prospective pereon (Fig. 3d), thus making the segmental character of the anterior post-naupliar region more defined. The segment of maxilla 1 is delayed in its development. More posteriorly, the ectodermal post-naupliar region still shows the regular, grid-like pattern of rows of cells and the segmentation process is still ongoing. During this stage of development, the dorsal half of the embryo consists entirely of a thin layer of large, yolky cells known as extra-embryonic tissue. Crossing over antenna 2, mandible and maxilla 1, the anlagen of the midgut form paired oval sacs which are open dorsally (Figs. 3d, e).

Limb buds pereon

The limb buds of antenna 2 and mandible are more prominent at this stage, but the protrusions are still small. Antenna 2 is about double the size of antenna 1. Segments of the first and second maxilla, maxilliped and the pereonic segments bear limb primordia as small ventrally pointed protrusions (Fig. 3g). Posteriorly, the ectoteloblasts still generate genealogical units which lead the embryo to elongate. Because of its ventral convex flexure, the embryo becomes C-shaped around the yolky mass.

Stomodaeum

The naupliar appendages show a higher degree of differentiation. Antenna 1 is very small. Antenna 2 points laterally and is two to three times longer than the mandible (Figs. 4a, b). The stomodaeum is formed slightly posteriorly to the

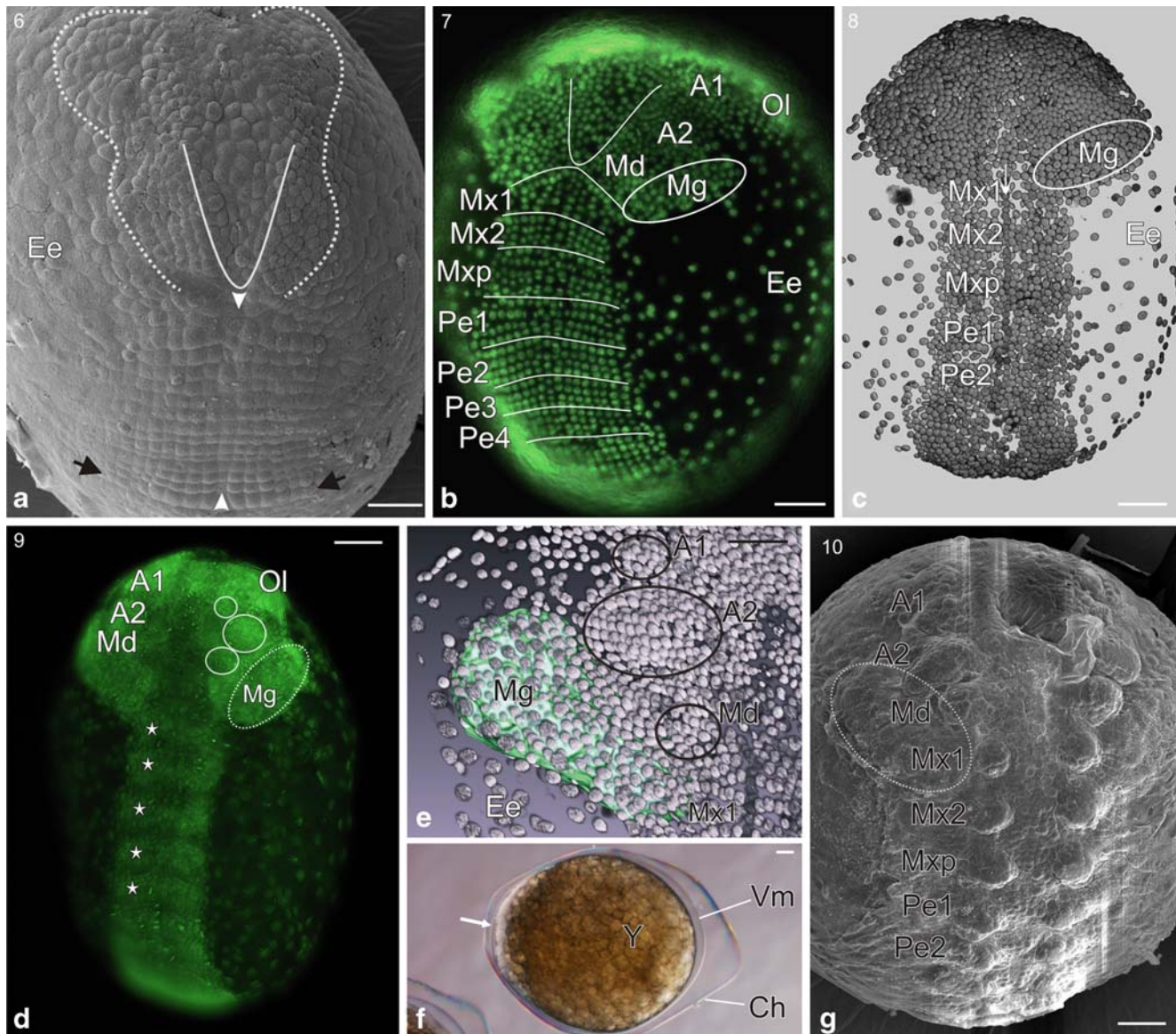


Fig. 3 Stages 6–10 of *P. scaber*. Ventral view unless indicated, anterior is up. All scale bars show 50 μm . **a** Stage 6, germ band. The ectoteloblasts (black arrows) generate more transverse rows which show a stereotyped cell division pattern. Medially, an unpaired row of cells represents the longitudinal midline (white arrowheads). The head region (dotted white lines) has a typical shape and is split into left and right part by a group of slightly sunken cells arranged in V-form (indicated by a white line). The surrounding extra-embryonic region (Ee) is loosely arranged and bigger cells. **b** Stage 7, midgut primordium. Nuclei-stained egg with a more advanced germ band as seen in **a**. The embryo is stretched along the *a-p*-axes and shows four head compartments (Ol optical lobes, A1 antenna 1, A2 antenna 2, Md mandible) and the post-naupliar ectoderm in a grid-patterned arrangement. The segmental anlagen of maxilla 1 (Mx1), maxilla 2 (Mx2), maxilliped (Mxp) and pereomers (Pe1–4) are indicated by white lines. **c** Stage 8, segment formation. 3D reconstruction of a confocal image stack of a nuclei-stained embryo. The midline (white

arrow) split the slightly bulged segments of maxilla 1 (Mx1), maxilla 2 (Mx2), maxilliped (Mxp) and first pereonic segments (Pe1–2) of the left and right body half. **d, e** Stage 9, naupliar appendages. **d** Nuclei-stained embryo with naupliar buds (indicated with white circles) of antenna 1 (A1), antenna 2 (A2) and mandible (Md). The posterior following segments (indicated with stars) are further developed and more distinct but still without limb buds. **e** 3D reconstructed confocal image stack (nuclei staining) of the right head region. The midgut primordium (Mg, artificially coloured green) is underneath a thin extra-embryonic layer (Ee) and forms a dorsally open pouch adjacent to antenna 2 (A2), mandible (Md) and maxilla 1 (Mx1). The bud of the antenna 1 (A1) is, compared to posterior following appendages, very small. **f** Embryo under normal light microscopy. The transparent embryonic tissue (white arrow) is on top of the yolky mass (Y) and hard to see. **g** Stage 10, limb buds pereon. The embryo shows small and narrow limb buds in its anterior segments (Mx1 maxilla1, Mx2 maxilla2, Mxp maxilliped, Pe1–2 pereon segments 1–2)

level of antenna 1. The surrounding tissue is formed by three conspicuous rims (one medial anterior and two postero-lateral) so that the opening has a typical Y shape (Figs. 4a, b). During further development, this formation moves subsequently into the stomodaeum. Maxilla 1 and maxilla 2 show no differentiation. The limb buds of all formed thoracopods (maxilliped and pereopods 1–6) have a homogeneous composition and start to differentiate. They are elongated and on their proximo-lateral part is a small additional protrusion which represents a vestigial exopod (Fig. 4a). Also, their prospective tergites are visible adjacent to the extra-embryonic yolky cells. At the seventh pereomere, limb buds are not detectable. The ectoteloblasts are no longer visible at this stage, and the generation of cell material is completed, but the differentiation within proper segments is still in progress. Posterior to the sixth pleomere, a seventh vestigial set of ectodermal cells is clearly noticeable.

Limb buds pleon

The naupliar region shows two prominent antero-lateral head lobes that are followed posteriorly by well-pronounced appendages (Fig. 4d). Instead of the tripartite rim surrounding the stomodaeum, the anlage of the labrum appears as paired epidermal protuberances fronto-laterally to the stomodaeum (Fig. 4d). The midgut primordia are completely closed and appear more dorsally (Fig. 4e). Initially, the closed midgut primordium shows a characteristic partition into three equally sized lobes. Shortly after this, the tripartition and little spherical bulbs are visible (Fig. 4f). They contain approximately 10% of the yolk which has developed a finer structure and appears darker than the outside yolk granules (Figs. 4c, e, f). The uniramous pereopods start to differentiate into proximal coxal parts and distal elongated parts which laterally bear the vestigial exopodal bud. Because of the developmental gradient along the anterior–posterior axes, this sequence of differentiation is comprehensible (Fig. 4a, j). The anterior-most pleopod buds start to develop, whilst the intersegmental furrows of the following pleomeres are about to differentiate. Shortly after outgrowth, a longitudinal depression along the distal bud indicates the subdivision into an outer exopod and inner endopod (Fig. 4g). The proctodeum is formed posterior to the sixth pleonic segment.

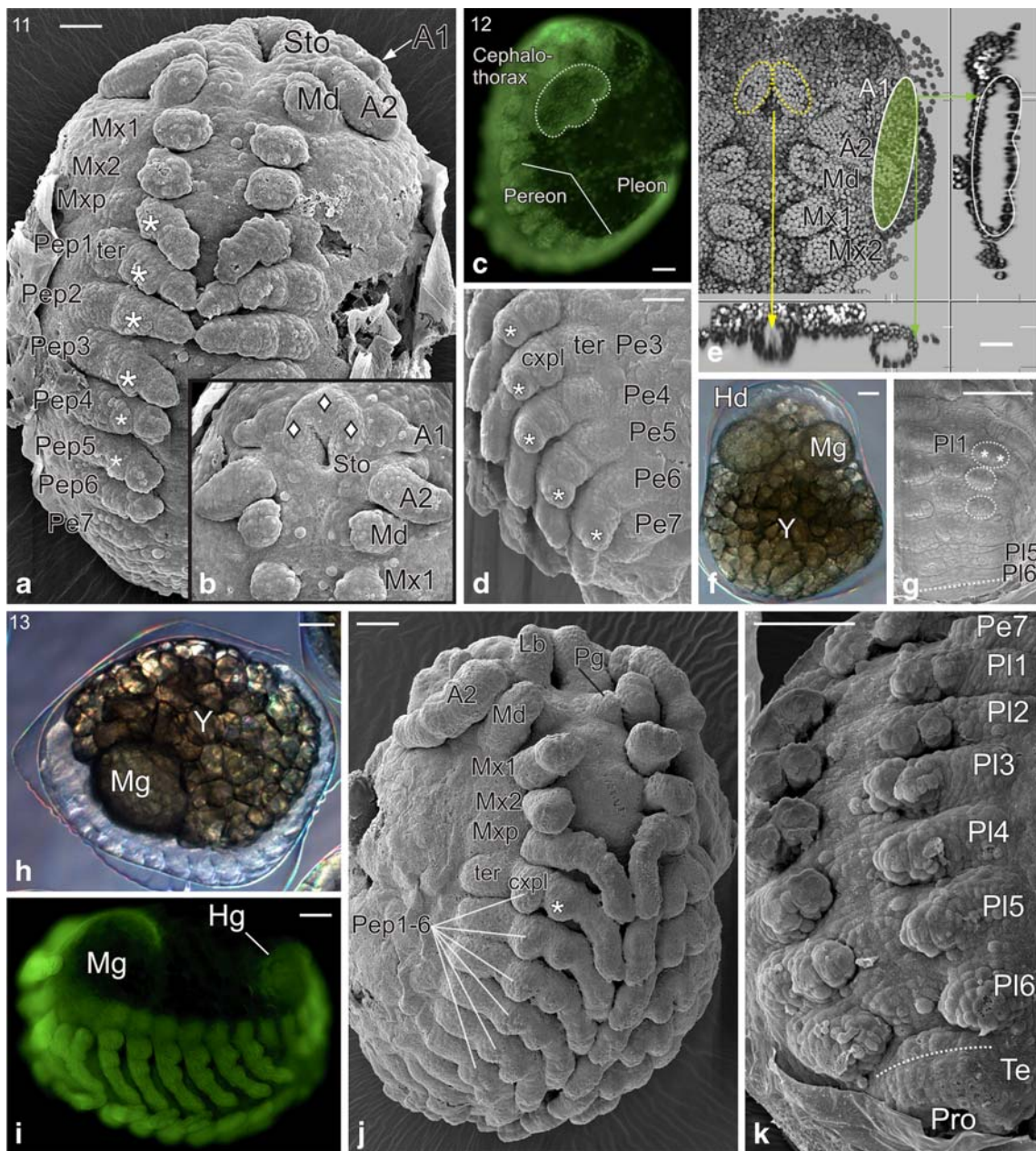
Fused labrum

The transparent embryo is more detached from the extra-embryonic yolk and now is more easily visible under light microscope (Fig. 4h). The two dorso-lateral midgut primordia are dorso-medially fused and now contain approximately 30% of the total yolky mass (Figs. 4h, i). The second

antenna becomes further elongated and starts to divide into its prospective segments (Fig. 4j). The two previously separated lobes of the labrum anlage are elongated, medially fused and point characteristically toward an anterior direction (Fig. 4j). This prominent unpaired structure is slightly shifted posteriorly and is now positioned at the level of antenna 2. Paragnaths humps grow out of the mandibular sternal region, close to the postero-medial base of the still undifferentiated mandible (Fig. 4j). Maxilla 1 develops a central longitudinal depression that gives it a bilobate shape. Maxilla 2 is still undifferentiated. Uniramous thoracopods 1–7 (maxilliped and pereopods 1–6) are more elongated but still unsegmented so that they join medially and point posteriorly (Fig. 4j). The vestigial exopodal buds decrease in size, and it seems that they become integrated laterally into limb structures. The pereonic anlagen of the tergites start with their further elongation to enclose the dorso-lateral extra-embryonic region. The seventh pereomere still shows no limb bud, but a broader anlage of the tergite. A cylindrical-shaped telson has formed and bears the proctodeum on its terminal end. The conspicuous vestigial bulge of the seventh pleonic segment is incorporated in telson and forms there the proximo-anterior part (Fig. 4k).

Head capsule

The embryo is less dorsally curved and in the course of the initial process of tagmatisation; the head capsule differentiates and encloses antenna 1 and antenna 2 (Figs. 5a, b). Three paired structures are noticeable which probably represent future brain parts such as the optic lobes, protocerebrum and deutocerebrum. Antenna 1 is three-segmented and points toward a latero-ventral direction whilst the six-segmented antenna 2 is about ten times longer and points toward a posterior direction. Medial to antenna 1 and antenna 2, the tectiform labrum anlage points anteriorly but has a more upright position. The midgut primordia now contain approximately 50% of the total yolky mass and a posterior extension results in a teardrop shape (Fig. 5a). The elongated thoracopods 1–7 (maxilliped and pereopods 1–6) start to divide into the seven podomeres (coxa, basis, ischium, merus, carpus, propodus and dactylus). The maxilliped is shifted medially, and the podomeres are smaller than in the pereopods. On its proximo-lateral area, an epipod develops and points laterally. The coxal plates of pereopods 1–6 are enlarged and cover the coxal segment (Fig. 5d). The six pairs of pleopods are about the same size and show a differentiation into a compact proximal protopod and two lobate rami that represent the endopods and exopods (Figs. 5a, c). The orientation of endopod and exopod of the last pleopods has changed from medial–lateral to anterior–posterior. Laterally adjacent to the protopods, the anlagen of



the tergites is formed (Figs. 5a, c). The cylindrical telson anlage is more prominent (Fig. 5c). The vestigial seventh segment is still visible but more integrated into the proximo-anterior telson anlage (Fig. 5e). About 30 cells form a medial bulge which is reminiscent of a ganglia anlage of more anterior segments.

Maxilliped differentiation

The course of tagmatization continues, and cephalothorax, pereon and pleon are discernible (Fig. 5e). At the base of maxilla 1, a squat endite differentiates. The midgut primordium has increased its size and contains approxi-

mately 70% of the total yolk mass (Fig. 5f). Frequent contractions of the posterior midgut tubes are observable (see [Supplementary material](#)). Dorsally, in between the midgut primordia, the dorsal organ is visible under light microscopy and is in contact with the egg shells (Figs. 5f, h). The pereonic tergites are further expanded dorsally and show a small overlap with the posterior following tergite. Lateral to the tergites, a conspicuous line of cells is visible in nuclei staining. This line shows no segmental pattern and probably represents the growth zone for the dorsal embryonic tissue. The coxal plates are distally slightly elongated and flattened. The seventh pereomere just shows a small tergite but also a remnant of a coxal plate. The

Fig. 4 Stages 11–13. All *scale bars* show 50 μm . **a–b** Stage 11, Stomodaeum. **a** Embryo in ventral view. The limb buds of the thoracopods (maxilliped (*Mxp*) and pereopods 1–6 (*Pep1–6*)) are elongated and show first differentiations. On their proximo-lateral area, little protrusions (indicated by *white asterisks*) are visible. Because of the developmental gradient, the sixth pereonic limb shows the least elongation. Laterally, adjacent to the limbs anlagen, the anlagen of the tergites (*ter*) occur. The seventh pereonic segment (*Pe7*) and the following pleonic segments lack limb buds. **b** Head region of the same embryo as in **a**. At the level of first antenna (*Al*), three stomodaeal projections (indicated by *white diamonds*) surround the Y-shaped stomodaeum (*Sto*). **c–f** Stage 12, limb buds pleon. **c** Lateral view of a nuclei-stained embryo with a characteristic C-shape. It shows a gradual development from anterior to posterior (future tagmata are indicated). Note that the well-developed midgut primordium shows a tripartition (*white dotted line*). **d** Lateral view of a pereonic region. The limb differentiation continued, and proximal small anlage of the coxal plates (*cxpl*) has formed. Distally adjacent lateral vestigial exopod (*white asterisk*) is more pronounced. **e** 3D reconstruction of a head region in ventral view. The left midgut primordium is highlighted with *green*. The small images show a longitudinal (*right*) and horizontal (*below*) section and illustrate that the midgut primordium (*green arrows*) is totally closed now and has a tubelike shape. The stomodaeal projections (indicated by *yellow arrows*) moved inwards, and the paired labral anlage (indicated by *yellow dotted lines*) appears anterior to the mouth opening. **f** Living embryo under normal light microscopy in dorsal view. Posterior to the head (*Hd*), two spherical midgut anlagen (*Mg*) contain about 10% of the total yolky mass (*Y*). **g** Ventral view of the pleonic region with first visible limb buds (*encircled with dotted white lines*). The bud of pleopod 1 shows already the separation into an inner endopod and outer exopod (*white asterisks*). Behind the sixth pleomere (indicated by a *white dotted line*), four to five rows of cells are visible and represent a vestigial seventh pleomere. **h–j** Stage 13, fused labrum. **h** Living embryo under normal light in lateral view. The transparent embryo stretches around the extra-embryonic yolk (*Y*), and the midgut anlage (*Mg*) contains about 30% of the total yolky mass. **i** Nuclei-stained embryo in ventro-lateral view. The hindgut (*Hg*) is shining through the yolk. **j** Ventro-lateral view. The prominent and bilobed labrum is dorsally fused and point into anterior direction. Postero-medially to the mandible (*Md*), the paragnaths (*Pg*) bulge out of the sternal region. **k** Pleon in latero-ventral view. The pleopods of pleomeres 1–3 (*Pl1–3*) show already the bilobed character, whilst the last pleomere (*Pl6*) shows just undivided limb buds. Posterior to pleomere 6, the vestigial seventh pleomere (indicated by a *white dotted line*) is involved in the formation of the telson which bears the proctodeum (*Pro*)

pleopods show laterally positioned coxal plates which, on pleopods 2–6, are almost the same size as the medially adjacent endopod. The endopod and exopod of the first pleopod are dramatically reduced in size whilst exopods of pleopods 3–5 are slightly enlarged. The vestigial seventh segment is entirely merged with the telson anlage (Fig. 5h). Starting at the anterior of the proctodeum, the hindgut begins to grow out in a straight, anterior direction (Fig. 5e).

Reduction of first pleopod

The pleonic region of the embryo turns more ventrally (Fig. 6a). The head capsule encloses all head segments including the maxillipeds, and the cephalothorax becomes

uncoupled from the neighbouring pereon. The now four-segmented maxillipeds move more medially and have a more upright position like all other head appendages (Fig. 6c). The paired midgut primordium is posteriorly elongated and has developed a more tube-like form. At this time, it contains approximately 90% of the total yolky mass; just a small amount which is joined with the dorsal organ lies external. Attached to the proctodeum, the hindgut grows out more and more in an anterior direction. At this stage, it has achieved at least 30% of the future total length of the hindgut (Fig. 6b). There is a smooth transition from the coxal plates to the enlarged tergites (Figs. 6a, d). The limb segments are elongated but still have a spherical appearance. The hemi-tergites of the last pleonic segments fuse dorso-medially and initiate the dorsal closure from posterior to anterior. The coxal plates of pleopods 3–5 have a cone-like shape. The first pleopods have disappeared, and the endopods of pleopod 2 are reduced dramatically in size (Figs. 6d, e). The conformation of pleopods 3–5 eventually changes when the bigger endopods start to move behind the corresponding exopods (Fig. 6e). The last pleopods (uropods) are noticeably larger than the others, their endopods and exopods rotated about 90° so that the endopods lay anterior and the exopods posterior.

Dorsal closure pleon

The pleonic region loses dorsal flexion, and the embryo turns into a more or less straight form. Because of the increased embryonic volume, the chorion ruptures, and the embryo becomes coated in only a vitelline membrane. The heart beats sporadically; the pereopods move in an uncoordinated manner, and the eyes show first pigmentation. Whilst all the head appendages move closer together, the cephalothorax becomes more compact (Figs. 6f, g). The paragnaths have a more medial position posterior to the mouth opening. The mandible and the first maxilla have a lateral position, whilst the second maxilla is inserted slightly more medially. Both maxillae show a weak expression of a distal subdivision into an inner and an outer endite (Fig. 6f). The two tubes of the midgut primordium which fill up most of the embryo now contain approximately 95% of the total yolky mass. Only some droplets of yolk are outside of the midgut (Fig. 6h). A second pair of midgut tubes starts to grow out medial to the already-differentiated tubular glands. Between the midgut anlage, the tubular hindgut lies as a straight strand and joins anteriorly with the foregut (Fig. 6j). The coxal plates of pereopods 5 and 6 are posteriorly elongated and show the differentiation of epimeres. The basis of pereopods 1–6 is elongated and much longer than the more distal limb segments. First pleomere shows only little bumps in the ventral limb region which can be

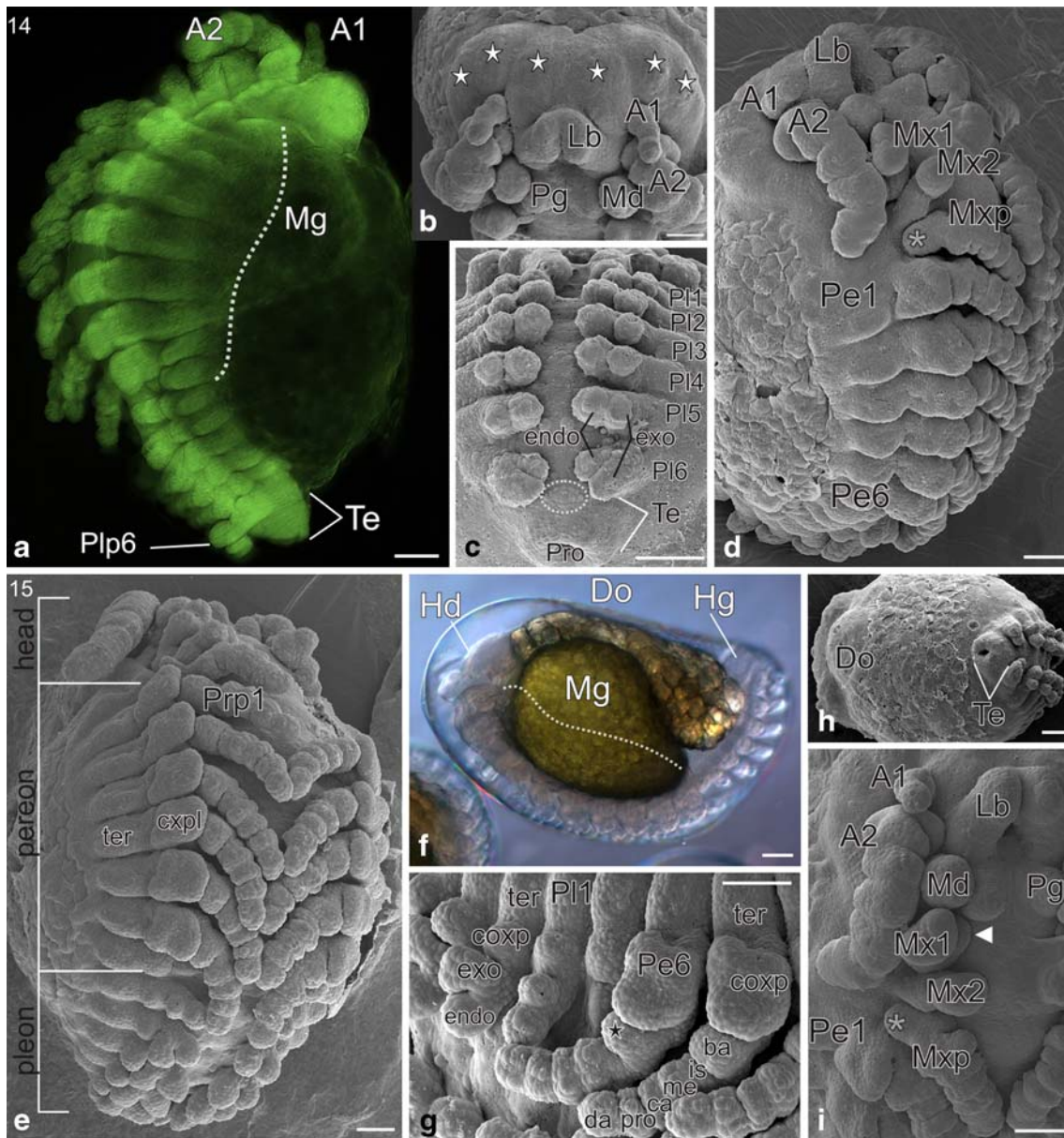


Fig. 5 Stages 14–15 of *P. scaber*. All scale bars show 50 μm . **a–d** Stage 14, head capsule. **a** Nuclei-stained embryo in lateral view. A head capsule is formed and encloses antenna 1 (*A1*) and antenna 2 (*A2*). The midgut primordia (*Mg*) have a more tear drop shape and increase their size. Pereonic tissue (indicated by a white dotted line) grows in lateral direction. The last pair of pleopods (*Plp6*) is bigger than the previous pleopods, and the telson (*Te*) is more pronounced. **b** Frontal view of a head with three distinct regions (white stars) of the future brain compartments. The strongly sclerotised head capsule encloses antenna 1 (*A1*) and antenna 2 (*A2*). The following head appendages like labrum (*Lb*), mandible (*Md*) and paragnaths (*Pg*) are more pronounced. **c** Ventral view of the pleonic region with bilobed pleopodal buds on each pleonic segment (*PI1–6*). The two branches represent the inner endopod (*endo*) and the outer exopod (*exo*). The seventh vestigial segment (indicated by white dotted line) is anteriorly incorporated in the telson (*Te*) which bears the proctodeum (*Pro*). **d** Lateral view of an embryo with segmented maxilliped and pereopods. The anlagen of the tergites and coxal plates are more pronounced. **e–i** Stage 15, maxilliped differentiation. **e** Ventro-lateral view of an embryo which shows distinct tagmata. The limb segments are slightly

elongated, and tergite (*ter*) and coxal plate (*cxpl*) start to form the fused complex. **f** Living embryo under normal light in lateral view. The midgut primordia contract and contain about 70% of the total yolk (see Suppl. material). The dotted line indicated the pereonic tissue which grows close to the embryo dorsally (*Hd* head, *Hg* hindgut, *Do* dorsal organ). **g** Lateral view of last pereonic and first pleonic segments. At the pereopod 6, the vestigial exopod (black star) is still visible. At the pleonic segments, anlagen of tergites (*ter*) and coxal plates (*cxpl*) are visible. Whilst the second pleopod shows proper endopod (*endo*) and exopod (*exo*), the first pleopod is dramatically reduced in size. (*ter* tergite, *cxpl* coxal plate, *ba* basis, *is* ischium, *me* merus, *ca* carpus, *pro* propodus, *da* dactylus). **h** Embryo in dorsal view. The dorsal organ (*Do*) appears like a hunchback, and the telson is projecting dorsally. **i** Head in ventral view. The prominent labrum (*Lb*) points anteriorly. The six-segmented antenna 2 (*A2*) is about seven times longer and much broader than the little antenna 1 (*A1*). An endite lobe (white arrow head) at maxilla 1 (*Mx1*) is noticeable, and the distant exite (grey asterisk) of the maxilliped (*Mxp*) points laterally. (*Md* mandible, *Pg* paragnaths, *Pe* pereomere 1)

interpreted as protopodial remnants. Each of the second pleopods has a distinct and broad protopod and a medially pointing exopod. The endopod is lacking. Laterally on the protopod, a little protrusion is visible which can be interpreted as a vestigial exite. At pleopods 3 to 5, the flap-like endopod is positioned behind the corresponding slightly smaller exopod. The cone-shaped epimeres of the tergites are more distinct.

Dorsal closure pereon (pre-hatchling)

The pre-hatchling is about 1.2 mm in length (from head to pleotelson), and its appearance has changed dramatically from a ventrally convex flexure to a ventrally concave flexure (Figs. 7a–c). The embryo exhibits the compact cephalothorax, the massive pereon and the pleon with the tail-like pleotelson (Figs. 7a, b, d). The mandible now shows differentiation of a distal incisor and a proximal molar process. No extra-embryonic yolk is left, and the second pair of midgut primordium is further elongated in a posterior direction. Pereonic limbs at this stage are more elongated. The podomeres have lost their spherical shape and show the proportions of the future juvenile's uniramous leg. Epimeres are differentiated on pereopods 1–6. The pereonic hemi-tergites of both body halves meet and fuse dorsally and complete the dorsal closure (Fig. 7c). At pleopods 3 to 5, the slightly swollen endopod is positioned behind the corresponding flap-like exopod. The enclosing cuticle is much thinner and indicates its differentiation into gills. The cone-shaped outgrowths of the tergites are more distinct. Pleomere 6 fuses with the telson and forms the so-called pleotelson (Fig. 7e). It bears the uropods (sixth pleopods) which have a large protopod and an anterior endopod and a posterior exopod.

Manca stages

Hatched embryos within the brood pouch are called manca stages. For *Porcellio*, usually they stay inside the brood chamber for up to seven more days. Once they are flushed out of the marsupium, the hatchlings are quite active. They flex the whole body using the trunk musculature and also move the pereopods and pleopods frequently. The fused cephalothoracic segments form a compact cuticular and slightly posteriorly extended head capsule which covers the tiny first antenna 1 (Figs. 8b, e). The six-segmented antenna 2 points antero-ventrally. The massive, shield-like labrum is directed posteriorly, concealing the stomodaeum. Laterally, the mouth is demarcated by the strongly sclerotized mandible, with its proximo-medial broad molar process and the distally tapered incisor process. Postero-medially to the mandible,

the paragnaths form the posterior margin of the mouth opening. The first maxilla is composed of a short inner endite and a larger outer endite. The second maxilla is composed of just one long endite. The proximally fused maxillipeds contain, laterally on their coxae, a long and laterally separated exite. The basis bears, medially, a short endite and, distally, three more segments (of which the most distal segment is strongly reduced). A dorsal typhlosolis is present in the anterior hindgut. Due to the consumption of the yolk stock by the hatchling, the midgut becomes narrower. Viewed from the dorsal trough the tergites, at pereomeres 3–6, the primordial gonads are noticeable as conspicuous circularly arranged cells (Fig. 8a). The pereonic coxal segment, its coxal plate and the corresponding tergite are fused into one protective unit which is imbricated upon and connected to the posterior following unit. The pereopods 1–6 are uniramous and uniform in size and conformation. The seventh pereonic and first pleonic segment lack limbs and epimeres. The second pleomere has also no epimere. Its pleopod lacks the endopod and the exopod forms the operculum. The broad and foliate exopods of pleopods 3–5 totally cover the gill-like endopods. Uropods point directly posteriorly and have a long two-segmented exopod and a short endopod. Together with the telson, they form the tail-like pleotelson. The anus opening is positioned ventrally and covered by anal valves. There are at least two types of distinct manca stages that have clear morphological differences.

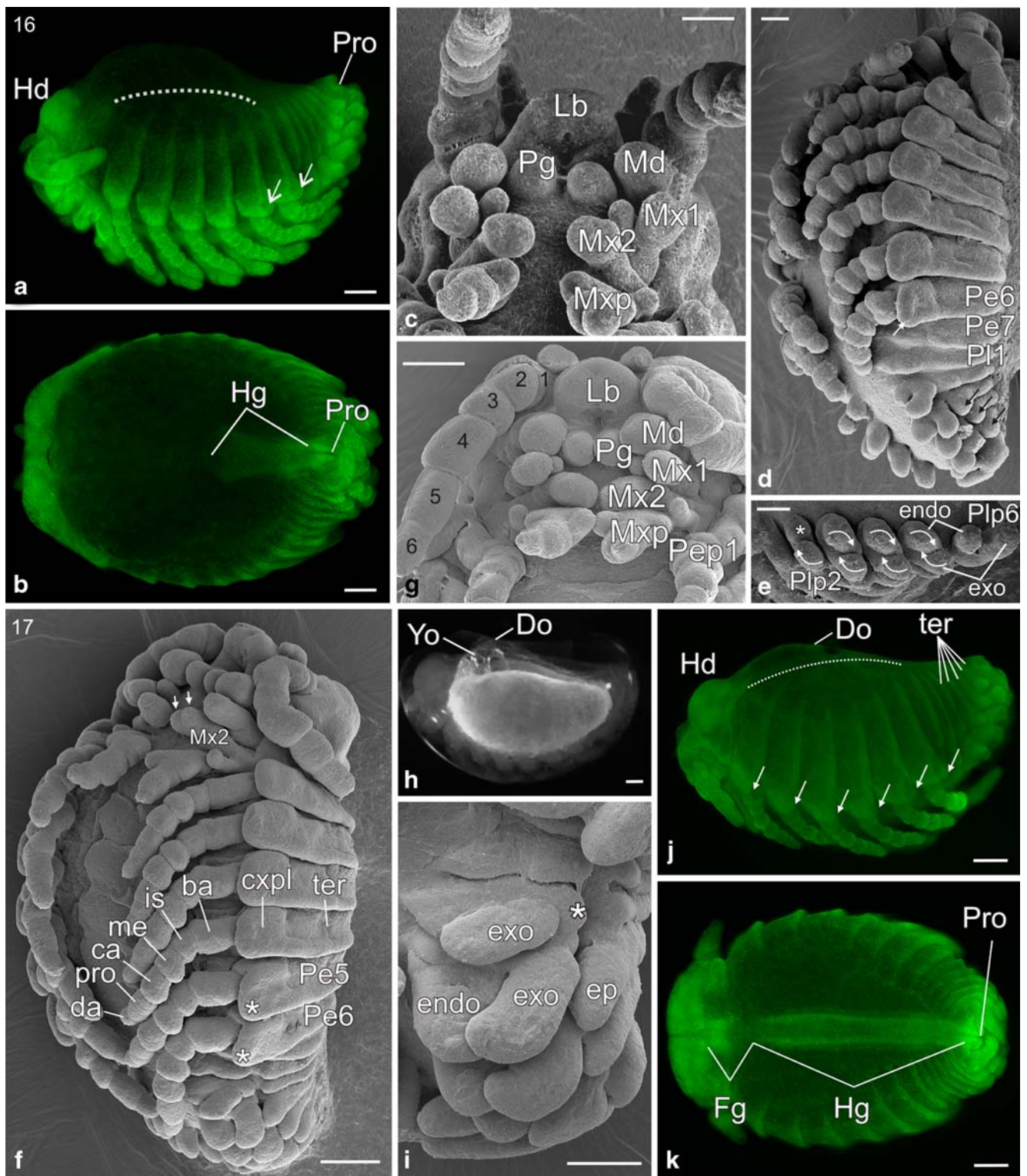
Manca 1

Animals of manca stage 1 are about 1.5 mm in length (from head to pleotelson).

The body is covered with prominent cuticular scales. The antenna 2 bears distally only a few setae (Fig. 8c). The sixth antennal segment bears a small flagellum (Fig. 8c). The distal border of the exopods of pleopods 3–5 bears long hairs that cover the posterior pleopods (Fig. 8d). Some hatchlings show less hair, but it is not clear whether they lose the hairy structure by moulting or not.

Manca 2

Manca stage 2 is about 1.7 mm in length (from head to pleotelson) and seems to be more relaxed than the previous stage. The cuticular scales are less prominent. The antenna 2 bears distally more setae than in the previous stage, and the flagellum is at least three times longer than the sixth antennal segment (Fig. 8b). Antenna 2 shows more setae on its distal segments (Fig. 8b), and the pleopods are free from hair tufts. At this stage, there is no external indication for the development of the seventh pair of pereopods.



Discussion

Previous developmental studies on *P. scaber* used the staging system of [Whittington et al. \(1993\)](#) which was based on the embryonic age. But unfortunately, there

are considerable differences in the developmental rate amongst the eggs of different broods. This study shows for the first time a complete and detailed sequence of the embryonic development of an isopod crustacean and will facilitate future developmental studies to define and to

Fig. 6 Embryonic stages 16–17. All *scale bars* show 50 μm . **a–e** Stage 16, reduction first pleopod. **a** Lateral view of a nuclei-stained embryo. The latero-dorsal growth zone of the pereonic tissue (indicated by the *dotted white line*) forms an almost straight line between the massive head capsule (*Hd*) and the proctodeum (*Pro*). The pleonic hemi-tergites (*ter*) of each body half are almost in touch. **b** Dorsal view of the same embryo as in **a**. Starting from the proctodeum (*Pro*), the hindgut (*Hg*) grows straight-lined in anterior direction. **c** Ventral of the head region. All cephalic feeding appendages (*Lb* labrum, *Md* mandible, *Pg* paragnaths, *Mx1* maxilla1, *Mx2* maxilla2) and the maxilliped (*Mxp*) moved medially together. **d** Lateral view. In addition to the seventh pereopod (*Prp7*), the first pleopod (*Plp1*) is lacking. At the posterior margin of the coxal plate of the sixth pereopod (*Prp6*), epimeres start to differentiate (indicated by a *white arrow*). At pleomeres 3–5, the coxal plates (indicated by *black arrows*) become a cone-like shape. **e** Ventral view of the pleopods. The endopod of pleopod 2 is strongly reduced in size. The transformation of conformation of endopods and exopods at pleopods 3–5 is indicated by the *white arrows*. Pleopod 6 (*Plp6*) rotates at about 90° that the exopod points not laterally but posteriorly. **f–k** Stage 17, dorsal closure pleon. **f** Vento-lateral view. Maxilla 2 (*Mx2*) show two distal lobes (*white arrows*). The basis (*ba*) of pereopods is much longer than the distal following podomeres (*is* ischium, *me* merus, *ca* carpus, *pro* propodus, *da* dactylus). Epimere differentiation continues (*white asterisks* at pereomeres 5 and 6 (*Pe5–6*)). **g** Head in ventral view. The head appendages are more joined together around the mouth opening. The maxillipeds (*Mxp*) are almost touching each other medially. **h** Lateral view under normal light microscope. Only view droplets of yolk (*Yo*) are outside the long midgut tubes. **i** Left pleonic region in ventral view. The exopods (*exo*) of pleopods 3–5 increase their surface and start to cover the endopods (*endo*). On the broad protopod of the second pleopod, only an exopod and the remnant of an exite (*asterisk*) insert. Lateral to exopods 3–5, the more pronounced coxal plates show the starting differentiation into epimeres (*ep*). **j** Lateral view of a nuclei-stained embryo. The latero-dorsal growth zone of the pereonic tissue (indicated by the *dotted white line*) forms an almost straight line between the massive head capsule (*Hd*) and the proctodeum (*Pro*). The pleonic tergites (*ter*) are dorsally fused, and the dorsal closure is complete. The pereonic hemi-tergites of each body half are almost touching each other (indicated by a *white dotted line*). **k** Dorsal view of the same embryo as in **j**. With the connection of hindgut (*Hg*) and the foregut (*Fg*), the formation of digestion apparatus is complete. (*Pro* proctodeum)

compare the different degrees of development of different structures.

A series of 20 discrete stages, easily identified by examination of living animals, will assist future work (Fig. 9). The findings of the present study regarding the development of *P. scaber* largely agree with previous data, e.g. adult morphology of isopods in general and their embryonic development. Besides its usefulness as a basis for future studies, certain aspects of the embryonic development make this species particularly interesting for future studies.

Cleavage and gastrulation of *P. scaber*

That isopods have yolky eggs and undergo a intralecithal superficial cleavage is reported by several authors (Dohrn 1866; Hahnenkamp 1974; Kajishima 1952; McMurrich 1895; Nair 1956; Nusbaum 1891; Strömberg 1965, 1967,

1972). Only some parasitic isopods (Epicaridea) have small yolkless eggs that show a total cleavage or an intermediate mode (Strömberg 1971). The changes of cleavage from total (holoblastic) to superficial (meroblastic) mode or vice versa are often believed to be related to the size and the yolk content of the eggs (e.g. Strömberg 1971). However, examples like the total cleavage of the yolk-rich eggs of amphipod crustaceans show that there is no such simple correlation between egg size, amount of yolk and type of cleavage (Scholtz and Wolff 2002). Although many studies of the early development exist (e.g. Anderson 1973), until today, we are at present unable to say which type of cleavage we can assume for the ground pattern of the Crustacea (Scholtz 1997).

The preceding facts do not necessarily mean that a superficial cleavage cannot have a distinct division pattern. The water flea *Leptodora kindtii* undergoes a superficial cleavage but shows a strict arrangement of the nuclei, which form two distinct cell bands (Samter 1900; Gerberding 1994). The water flea *Bythotrephes* shows an intermediate type of cleavage. Until the fourth division, cell membranes are only formed at the egg surface, and the blastomeres are not completely separated from each other (Alwes 2008). However, up to the fifth cell division cycle, the cell division pattern is stereotyped and shows striking similarities to division patterns of total-cleaving malacostracan crustaceans (Alwes 2008).

Interestingly, there is a strict nucleus arrangement observable in a four-nuclei stage and probably in the eight-nuclei stage. Out of the two nuclei, the spindle orientation is oblique to each other that the four nuclei form together a tetrahedron. The next (third) cleavage is perpendicular to the previous cleavage, and all nuclei are equally distributed within the egg. This is already described for several isopods (*Idotea*: Strömberg 1965; *Limnoria*: Strömberg 1967; *Bopyroides*: Strömberg 1971). During the third and fifth cleavages, the energids (nuclei with surrounding protoplasm) move towards the surface; they stop cleaving simultaneously and start to form the germ disc. With the methods used for this study, it was not possible to trace further cleavages to determine whether or not there is a cell lineage pattern of building a germ disc. For this reason, this issue must remain unresolved at present. A solution to this problem lies in further studies applying suitable methods, such as 4D microscopy, in order to trace cell lineages of single blastomeres.

Stomodaeum formation

The formation of the mouth region takes place in two distinct phases. The first phase is the development of the mouth opening surrounded by three stomodaeal projections. A similar process is also described for amphipods where

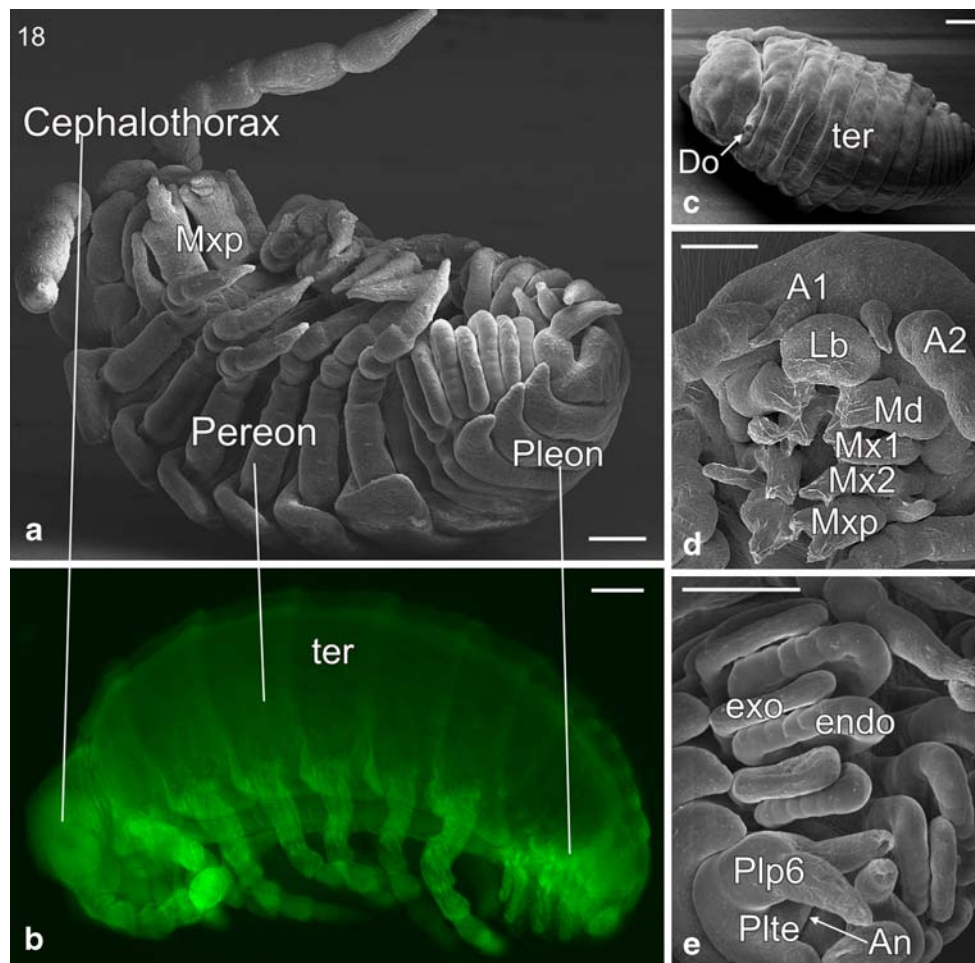


Fig. 7 Stage 18, dorsal closure pereon. All scale bars show 100 μm . **a** Ventrally bended pre-hatchling in latero-ventral view. The prominent maxillipeds (*Mxp*) form a clear border between cephalothorax and pereon. **b** Nuclei-stained embryo in lateral view. The pereonic tergite (*ter*) formation is done, and dorsal closure is complete. **c** Dorsal view of an embryo. Between the cephalothorax and the pereon, remnants of the dorsal organ (*Do*) are still attached to the embryo. **d** Compact cephalothorax in ventral view. The mouthparts (*Lb* labrum, *Md* mandible, *Pg* paragnath, *Mx1* maxilla 1, *Mx2* maxilla 2, *Mxp*

maxillipeds) are further differentiated and concerted, e.g. the mandible (*Md*) shows a differentiation into a proximal molar and a distal incisor part. The embryo is covered by a thin cuticular membrane. **e** Pleonic region in ventral view shows the further differentiation of the pleopods. The bloated and endopods (*endo*) are almost totally covered by the corresponding exopods (*exo*) and show that its cuticle is strikingly thin-skinned. The last pleomere bears large uropods (*Plp6*) together with the telson and forms the so-called pleotelson (*Plte*) which bears postero-ventrally the anus opening

these projections move subsequently into the developing mouth and form main parts of the oesophagus (Weygoldt 1958; Ungerer and Wolff 2005). Due to the array of the stomodaeal projections (one anterior and two laterals), the mouth opening assumes a characteristic triangular shape (Y shape). The second event is the formation of the labral anlage. Therefore, at the anterior margin of the stomodaeum, two separated humps bulge out and fuse medially during ongoing development. The unpaired labrum increases in size, bends ventrally and finally covers the mouth opening. Interestingly, this characteristic shape of the stomodaeal opening has been shown in spiders (Liu et al. 2009) and in pycnogonids (Morgan 1891; Jakob Machner personal communication). But there is a difference. At least in spiders, the triangular mouth opening

is caused by one medial stomodaeum pore and two lateral invagination sites (local spots of early neurogenesis) and is not, like in crustaceans, formed laterally by stomodaeal projections. A Y-shaped stomodaeal opening and its posterior migration during head formation probably represent a homoplastic feature amongst arthropods. Future comparative studies on the formation and differentiation of the stomodaeum in several arthropod species could contribute to this matter.

Digestive system

A complex ectodermal digestive tract with a well-developed typhlosolis to recycle fluids is an important adaptation to terrestrial life (Hames and Hopkin 1989; Strus

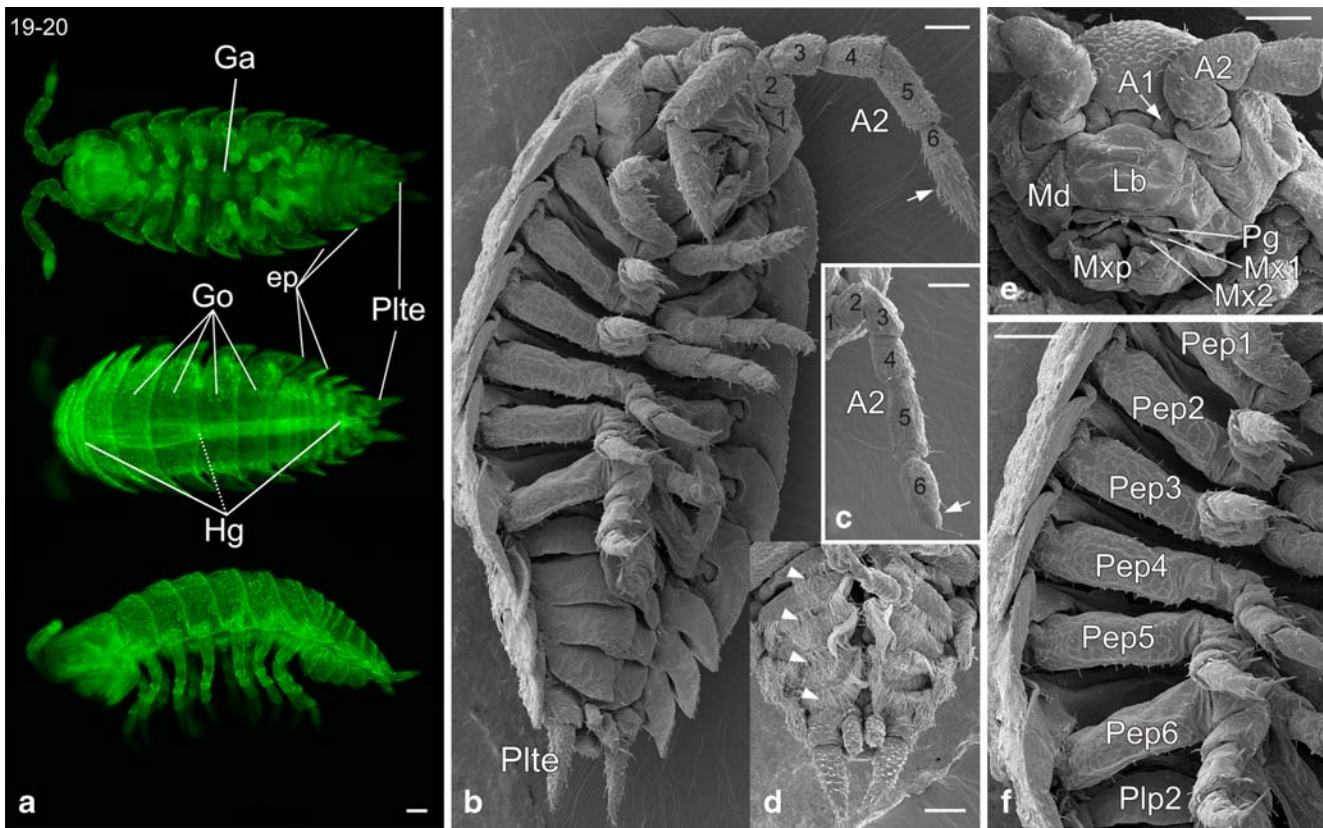


Fig. 8 Stages 19–20, manca stages of *P. scaber*. All scale bars show 100 μ m. **a** Ventral, dorsal and lateral view of a nuclei-stained manca larva 2. Structures like epimeres (*ep*) or pleotelson (*Plte*) become their final shape. Ventrally, the segmental ganglia (*Ga*) shine through the cuticle. The hindgut (*Hg*) shows a differentiation into an anterior and a posterior part (indicated by *white dotted line*). Latero-dorsally at pereomeres 3–6, circularly arranged cells represent the primordial gonads (*Go*). **b** Manca 2 stage with its typical features. The distal segments of antenna 2 (*A2*) shows a high number of sensory setae. The flagellum (*white arrow*) is much longer than the sixth antennal

segment. **c, d** Details of manca 1 stage. **c** The second antenna of manca 1 bears less setae on its distal segments, and the antennal flagellum (*white arrow*) is very short. **d** The exopods of pleopods 2–5 have hair tufts on the posterior ridge (*white arrows*). **e** Head of manca 2 in ventral view. The prominent second antenna (*A2*) covers partly the tiny antenna 1 (*A1*). All mouthparts (*Md* mandible, *Pg* paragnath, *Mx1* maxilla 1, *Mx2* maxilla 2) are concentrated and covered by the labrum (*Lb*). **f** Pereonic region (ventral view) of a manca 2 stage with fully developed pereopods (*Pep1*–*6*)

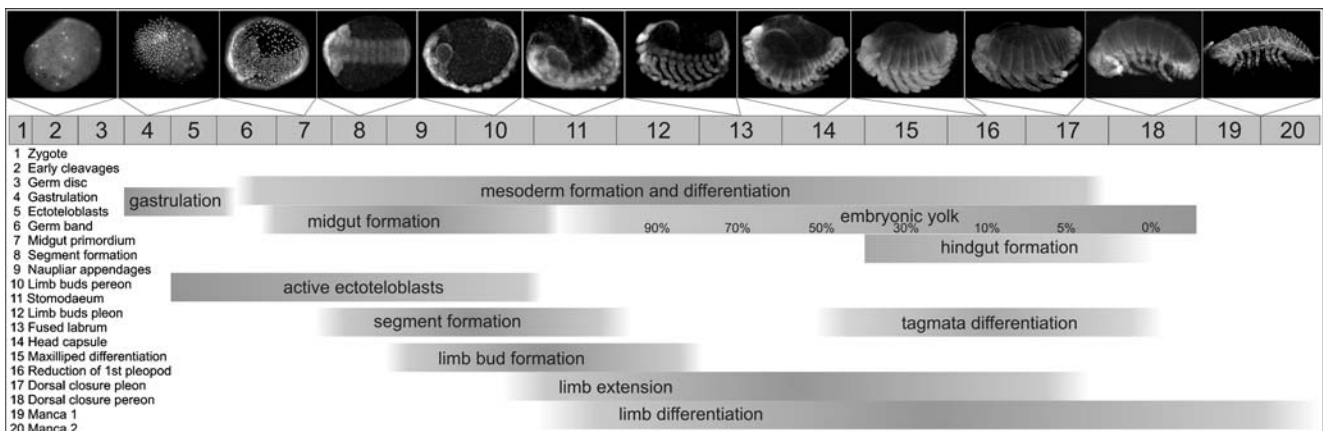


Fig. 9 Summary of the embryonic development of the woodlouse *P. scaber*. Nuclei-stained embryos show most of the total 20 stages of the embryonic development. Some important developmental events indicated by the *solid bar* (*faded areas* indicate uncertain start or end points)

et al. 1995). The morphogenesis of the digestive tract was studied by several authors (Bullar 1878; McMurrich 1895; Goodrich 1939; Nair 1956; Strömberg 1965, 1967; Strus et al. 2008). When Goodrich (1939) studied the embryonic development of *Porcellio laevis*, he showed in great detail that the digestive tract is exclusively an ectodermal formation of stomodaeum and proctodeum. The only endodermal element is the midgut primordium (= midgut glands, digestive caeca, hepatopancreas). They form elongated tubes which insert at the foregut–hindgut junction and reach to the last pereomere. This was confirmed by other authors and partly at ultra-structural level (Strömberg 1965, 1967; Holdich 1973; Wägele 1992; Strus et al. 2008). This study shows that the size and shape of the midgut primordium and the degree of hindgut differentiation are helpful and efficient tools to distinguish developmental stages of *Porcellio*.

Another interesting feature is the way of hindgut formation. Beginning at stage 15, the hindgut grows dramatically fast straight-lined in anterior direction to contact the stomodaeum. This is similar to what is described for *Drosophila*. Here, the hindgut is formed by self-renewing stem cells which generate the future hindgut tissue in anterior direction (Takashima et al. 2008). Maybe *Porcellio* as a crustacean offers the potential to give more insights in the complex field of stem cell research.

Pereon

An exceptional feature in terrestrial isopods (Oniscidea) is that the walking legs consist only of six limb segments. The most proximal podomere—the coxa—is not movable anymore and is totally fused with the body wall (Calman 1909; Gruner 1993). The isopod body wall is a very protective construction with dorso-laterally, flat overhanging keels—the so-called epimeres. For *Porcellio*, Gruner (1954) reported that the coxa transforms into an epimere structure, and together with the tergite as a fusion product, it forms the dorsal body wall. This study shows more precisely that the dorsal construct is a formation of tergite and coxal plate and not the coxa itself. Still it is not clear how the coxa is involved in the formation of the ventral body wall. How the ventral part is formed exactly and if and how the coxa is fused ventrally with the sternite need to be further investigated.

Pereopods

The uniramous pereopods and biramous pleopods in *Porcellio* have the same serially homologous origin in the post-naupliar cells formed by ectoteloblasts (Hejnal and Scholtz 2004). All buds, when they first appear, show one proximal–distal axis and have the same size and shape.

During outgrowth at stage 11, the thoracopods (maxilliped and pereopods 1–6) show on their lateral side an additional small bud that can be interpreted as a vestigial rudiment of an exopod. Throughout limb differentiation in stages 12–15, this transitory exopod shrinks more and more and gets laterally implemented into the second podomere (basis). The appearance of a transitory exopod in pereopods was already mentioned in older literature. Nusbaum (1891) showed it in an early stage of *Ligia*. McMurrich (1895) and Nair (1956) mentioned the appearance of a transitory exopod in their texts but they did not show it in their drawings. Regarding earlier studies, Strömberg made explicit the statement that “I have not been able find distinct lobation of the distal ends” of early pereopods in *Limnoria* (Strömberg 1967, p. 107). Recently, Jaume (2001) noted the presence of a small setose lobe on the basis of the fifth pereopods in *Atlantasellus*, and he interpreted it as a possible exopod. At first view, a transitory remnant of an exopod in *Porcellio* support the traditional idea view that uniramous crustacean limbs are generated by a reduction or a loss of exopods (Hansen 1925; Bitsch 2001). But the data are surprising since a recent study showed that uniramous pereopods are formed by a suppression of the split into an outer exopod and an inner endopod of the primary growth zone of the main limb axis (Wolff and Scholtz 2008). In a study of the clonal composition in the amphipod crustacean *Orchestia cavi-mana*, Wolff and Scholtz (2008) demonstrated that the same population of cells (out of the post-naupliar ectoderm) which forms the exopod in the biramous pleopods contributes to the outer part of the uniramous pereopods along most of the proximo-distal axis. Based on the finding, they offered a new criterion to discriminate different limb branches in arthropod appendages and considered—compared by recent and fossil data—that a “true” biramous limb (bearing an outer exopod and an inner endopod) evolved in the line of the Mandibulata or even the Tetraconata. On the contrary, the more traditional view places the biramous limb (with an outer exopod and an inner endopod) as a common feature for the Euarthropoda (Boxshall 2004; Boxshall and Jaume 2009). The available data for *Porcellio* show striking differences to what is described for the amphipod *Orchestia*, and it speaks rather for a reduction of the exopod or the suppression of its outgrowth and not for a developmental fusion of both rami into a common telopod. However, the data about the uniramous limb development in *Porcellio* support the idea of an initial limb axis forming an endopod and exopod whilst all other side branches like endites or exites are formed by secondary limb axis/axes. In the case of *Porcellio*, the anlagen of the coxal plates (exite) occurs later during limb differentiation and follows a secondary limb axis. Nevertheless, our knowledge of embryonic development of diverse crustacean limb morphologies is very partial, and there is a

general need for further studies. Using new high-quality morphological techniques but also molecular techniques in the future can shed more light upon this issue.

Pleon

At the time when the pleopods start their development (stage 12), a field of conspicuous ectodermal cells posteriorly adjacent to sixth pleomere is visible and is interpreted here as a vestigial seventh pleonic segment. This aspect is visible only for a short time when the germ band reaches its maximal extension and the ectotoloblasts stop their activity. Shortly after and due to the rapid process of segment formation in the pleon, this seventh segment is only visible as a medial bump of cells. Its appearance is reminiscent of an early ganglia anlage in more anterior segments. When the telson forms its cylindrical shape (beginning with stage 13), these cells get more and more merged into the telson anlage. This is the first observation for isopods that an additional segmental set of cells is formed posterior to the sixth pleonic segment. A seventh limbless pleonic segment is assumed to belong to the ground pattern of Malacostraca but is retained only in adult Leptostraca (Lauterbach 1975; Richter and Scholtz 2001). In fact, in most representatives of eumalacostracan taxa, traces of at least one more additional segment anlage posterior to pleomere 6 have been reported during embryogenesis (e.g. Hoplocarida: Shiino 1942; Syncarida: Hickman 1937; Decapoda: Scholtz 1995; Mysidacea: Manton 1928; Tanaidacea: Scholl 1963; Amphipoda: Ungerer and Wolff 2005). Possibly due to the rapid process of segment formation, there was no clear statement for isopods about a seventh pleonic segment. Although Strömberg (1967) did not note an additional seventh ectodermal segment in *Limmoria*, he observed an undersized seventh ganglia anterior adjacent to the proctodeum. However, Nair (1956) for *Irona* and Strömberg (1971) for several epicarids specifically noted that there are not more than six abdominal ganglia formed. Looking at α -tubulin-stained embryos, to see the axogenesis of the nervous system, I can confirm the appearance of a seventh ganglion very close to the proctodeum (unpublished data). Typical for isopod crustaceans is that they possess a pleotelson formed by the fusion of the telson and one to several pleomeres. In adults of *Porcellio*, a suture separates the telsonic part from the pleonic part in ventral view (Knopf et al. 2006). Due to the cuticle formation beginning with stage 18, it was impossible to look at the detailed formation of the pleotelson. Such a formation of a late embryonic or juvenile cuticle is already known for isopods but also for other crustaceans (Powell and Halcrow 1985; Ungerer and Wolff 2005; Havemann et al. 2008).

Pleopodal gills in Isopoda

In general, malacostracan gills are derivatives from different proximo-lateral elements of the pereopods (the epipods, the coxopods or even the pleura). However, decapod gills are derived from pereopodal epipods (or pleural extensions), whereas the gills of isopods are derived from the pleopodal endopods. Thus, they have a very different origin and are not homologous. Data from this study can properly show the process that the exopods of pleopods 3–5 cover the corresponding endopods which are transformed into branchial structures. In *Drosophila*, the tracheal system arises from cell clusters that express the tracheal inducer genes *tracheless* (*trh*) and *ventral veinless* (*vvl*; de Celis et al. 1995). Based on the similar expression pattern of *trh* and *vvl* in the gills of crustaceans, a common evolutionary origin of crustacean gills and insect tracheae has been suggested (Franch-Marro et al. 2006). Furthermore, the expression patterns of the genes *apterous* and *pdm/nubbin* lead to the assumption that out of an ancestral gill different terrestrial adaptations took place and that insect wings, breathing organs and spinnerets have a common evolutionary origin (Averof and Cohen 1997; Damen et al. 2002). In *Porcellio*, the gene *vvl* has a distinct expression at the endopods of pleopods 3–5 (Abzhanov and Kaufman 2000c). It supports the view that this gene is involved in the differentiation of crustacean respiratory organs, but regarding the idea that crustacean gills, insect wings and spider's spinnerets share a common origin, the *vvl* expression in *Porcellio* does not fit into this scenario. The *vvl* expression is not at lateral limb branch (epipod) but on the opposite side, the inner side of the pleopod. Furthermore, the Hox gene *Abdominal-B* plays a possible role in the differentiation of respiratory organs; thus, it is expressed in late stages of *Porcellio* exclusively in pleopods 3–5 (Brena et al. 2005). The authors stress that “the presence of those transcripts does not imply homology of these structures, but likely represents an independent co-option of these genes in broadly equivalent processes” (Brena et al. 2005).

Pleopodal epipods

Traditionally, the proximal segment of the pleopods of Malacostraca is interpreted as a fusion product of coxa and basis (Thiele 1905; Borradaile 1926) or a fusion product of a pre-coxa, a coxa and a basis (Hansen 1925). This is supported by several reports of pleopodal epipodites in malacostracans (see review of Boxshall and Jaume 2009). During development, the amphipod crustacean *Orchestia cavimana* shows a conspicuous subdivision in the pleopodal protopods which can be read as an originally segmented proximal limb part in the pleon. However, Walossek (1999, 2003) disagrees with this view and supposes a single

proximal segment in the pleopods formed exclusively by the basis. He claims that the proximal pleonic segment plesiomorphically does not consist of any coxal structures. In this line of arguments, pleopods in Malacostraca have an unsegmented protopod (called basis) without any additional side branches.

For the isopod taxa Phreatoicidea and Flabellifera, it is also considered that epipods occur in adults (Schram 1986; Wilson 2009). Snodgrass (1952) shows a lateral protrusion on the first and second pleopod of the oniscidean crustacean *Ligydia exotica* and calls it an epipod. However, a developmental confirmation that these lateral branches represent epipods or not was still missing. The sequential development of pereon and pleon shows in the pleon lateral structures which are serial homologous to the coxal plates (epipods) in the pereon. They occur in the same chronology as in the pereon (stage 15, after the first limb buds which represent the actual pleopods); as lateral protrusions at the proximal limb segments (coxae in pereon, protopods in pleon), they have the same location, and they have the same appearance. Furthermore (beginning in stage 16), these epipodal structures expand dorsoventrally and differentiate into epimeres in pleomeres 3–5. Finally, they fuse with the anlage of the tergite and form dorsally the same protective body wall which we know from the pereon. All these single features together leave no doubt about the presence of epipods in the pleon of *Porcellio*.

Manca stages and post-marsupial development

Two distinct manca stages inside the marsupium are observed in this study. This contradicts the general view of only one marsupial manca stage (Araujo et al. 2004; Brum and Araujo 2007). Interestingly, in both manca stages—neither in SEM nor with nuclei staining—no indication for the outgrowth of the seventh pereopod is given. Studies about manca development (Araujo et al. 2004; Brum and Araujo 2007) show that a differentiation of a seventh pereopod takes place in two consecutive post-marsupial stages. This is a support for two real marsupial manca stages instead of just one “real” marsupial manca stage and one manca stage—already bearing the anlage of the seventh pereopod—which is going to leave the marsupium. Furthermore, it has the consequence that in *Porcellio* we have in total at least four manca stages, two marsupial stages and two post-marsupial stages. This also fits the observations that during post-embryonic development of *P. scaber* the appearance of the seventh pereopod takes place in post-marsupial development (Tomescu and Craciun 1987, by their nomenclature, they call the stage with seventh pair of pereopods manca II stage). One remarkable characteristic for manca 1 is the

cuticular hairs at the distal margin of the exopods at pleopods 2 to 5. They cover the soft-skinned gills of pleopods 3 to 5. These tufts of hairy setae are already described for *Porcellio dilatatus* and are probably an adaptation to life inside the marsupium (Brum and Araujo 2007). Whether this structure gets lost by moulting or the juveniles just lose it during further development is not clear. Some SEM samples of larval stages showed a much lower number of exopodal hairs which were not strongly attached to the exopodal cuticle. It could be an indication that these hairy structures get lost without a moult, or it is just an artefact during SEM preparation. Other characteristics like the increasing number of sensory setae at the distal segments of antenna 2 and the extension of the distal article of antenna 2 display typical features during post-embryonic development in isopods (Brum and Araujo 2007; Tomescu and Craciun 1987).

When the development of the seventh pair of pereopods is completed, isopods are classified as juveniles, and the development of secondary sexual characteristics starts (Araujo et al. 2004). Oniscidean females carry the eggs in a brood pouch (marsupium), which is composed of oostegites projecting medially from the coxae of pereopods 1–5 (Gruner 1966). It has been widely assumed that oostegites are probably homologous to epipods (e.g. Hansen 1925; Gruner 1965). However, in keeping with the literature (e.g. Calman 1909; Gruner 1965), we did not find oostegites or theiranlagen during embryonic development. In *Asellus*, they appear as small buds from the coxa, increasing in size until maturity is reached. For some Oniscidea, it is reported that oostegites are visible externally after parturial moult (Calman 1909).

Males of *Porcellio* develop gonopods at the first and second pleomere at sexual maturity. At the first pleomere, the endopods are elongated and fuse proximo-medially, whilst at the second pleomere the endopods are elongated separately. This transformation takes place within three moulting steps during post-embryonic development (Tomescu and Craciun 1987, by their nomenclature from ‘juvenile stage phase 1’ until ‘adult stage’). Interesting here is the fact that during pleonic development the first pleomere reduces its pleopods completely, and the second pleomere develops the pleopodal exopods which represent the so-called opercula. All limb modifications like oostegites and gonopods which play an important role in reproduction take place within maturation.

Acknowledgements I thank R. Mbacke for the help with collecting specimens and G. Drescher (Natural History Museum, Berlin) for the support in using the SEM. I also thank Kristen Panfilio and the two reviewers for the helpful advice and Greg Edgecombe for improving the English.

References

- Abzhanov A, Kaufman TC (1999a) Homeotic genes and the arthropod head: expression patterns of the *labial*, *proboscipedia*, and *Deformed* genes in crustaceans and insects. *PNAS USA* 96:10224–10229
- Abzhanov A, Kaufman TC (1999b) Novel regulation of the homeotic gene *Scr* associated with a crustacean leg-to-maxilliped appendage transformation. *Development* 126:1121–1128
- Abzhanov A, Kaufman TC (2000a) Crustacean (malacostracan) Hox genes and the evolution of the arthropod trunk. *Development* 127:2239–2249
- Abzhanov A, Kaufman TC (2000b) Evolution of distinct expression patterns for *engrailed* paralogs in higher crustaceans (Malacostraca). *Dev Genes Evol* 210:493–506
- Abzhanov A, Kaufman TC (2000c) Homologs of *Drosophila* appendage genes in the patterning of arthropod limbs. *Dev Biol* 227:673–689
- Abzhanov A, Kaufman TC (2004) *Hox* genes and tagmatization of the higher Crustacea (Malacostraca). In: Scholtz G (ed) *Evolutionary developmental biology of Crustacea*. A.A. Balkema, Lisse, pp 43–71
- Alwes F (2008) Cell lineage studies in Crustacea—Aspects of the early development and germ layer formation in *Meganyctiphanes norvegica* (Malacostraca, Euphausiacea) and *Bythotrephes longimanus* (Cladocera, Branchiopoda). Humboldt-University Berlin. Ph.D. thesis, pp 109
- Anderson DT (1973) *Embryology and phylogeny in annelids and arthropods*. Pergamon, Oxford, p 495
- Araujo PB, Quadros AF, Augusto MM, Bond-Buckup G (2004) Postmarsupial development of *Atlantoscia floridana* (van Name, 1940) (Crustacea, Isopoda, Oniscidea): sexual differentiation and size at onset of sexual maturity. *Inv Repr Dev* 45:221–230
- Averof M, Cohen SM (1997) Evolutionary origin of insect wings from ancestral gills. *Nature* 385:627–630
- Bitsch J (2001) The hexapod appendage: basic structure, development and origin. *Ann Soc Entomol Fr (NS)* 37:175–193
- Borradaile LA (1926) Notes upon crustacean limbs. *Ann Mag Nat Hist Ser 9* 17(98):193–213
- Boxshall GA (2004) The evolution of arthropod limbs. *Biol Rev* 79:253–300
- Boxshall GA, Jaume D (2009) Exopodites, epipodites and gills in crustaceans. *Arth Syst Phyl* 67:229–254
- Brena C, Liu PZ, Minelli A, Kaufman TC (2005) *Abd-B* expression in *Porcellio scaber* Latreille, 1804 (Isopoda: Crustacea): conserved pattern versus novel roles in development and evolution. *Evol Dev* 7:42–50
- Browne WE, Price AL, Gerberding M, Patel NH (2005) Stages of embryonic development in the amphipod crustacean, *Parhyale hawaiensis*. *Genesis* 42:124–149
- Brum PED, Araujo PB (2007) The manca stages of *Porcellio dilatatus* Brandt (Crustacea, Isopoda, Oniscidea). *Rev Brasil Zool* 24:493–502
- Bullar JF (1878) On the development of the parasitic Isopoda. *Phil Trans Roy Soc London* 169:505–521
- Calman WT (1909) Crustacea. In: Lankester ER (ed) *A treatise on zoology*. Adam and Charles Black, London, p 346
- Campos-Ortega JA, Hartenstein V (1997) *The embryonic development of Drosophila melanogaster*. Springer, Berlin, p 405
- Damen WGM, Saridaki T, Averof M (2002) Diverse adaptations of an ancestral gill: a common evolutionary origin for wings, breathing organs, and spinnerets. *Cur Biol* 12:1711–1716
- de Celis JF, Llimargas M, Casanova J (1995) *Ventral veinless*, the gene encoding the Cfl a transcription factor, links positional information and cell differentiation during embryonic and imaginal development in *Drosophila melanogaster*. *Development* 121:3405–3416
- Dohle W, Scholtz G (1988) Clonal analysis of the crustacean segment: the discordance between genealogical and segmental borders. *Development Suppl* 104:147–160
- Dohle W, Scholtz G (1997) How far does cell lineage influence cell fate specification in crustacean embryos? *Sem Cell Dev Biol* 8:379–390
- Dohle W, Gerberding M, Hejnol A, Scholtz G (2004) Cell lineage, segment differentiation, and gene expression in crustaceans. In: Scholtz G (ed) *Evolutionary developmental biology of Crustacea*. Crustacean issues 15. A.A. Balkema, Lisse, pp 95–133
- Dohrn A (1866) Die embryonale Entwicklung des *Asellus aquaticus*. *Z Wiss Zool* 17:221–278
- Drobne D (1997) Terrestrial isopods—a good choice for toxicity testing of pollutants in the terrestrial environment. *Environ Toxicol Chem* 16:1159–1164
- Franch-Marro X, Martin N, Averof M, Casanova J (2006) Association of tracheal placodes with leg primordia in *Drosophila* and implications for the origin of insect tracheal systems. *Development* 133:785–790
- Gerberding M (1994) Superfizielle Furchung, Bildung des Keimstreifs und Differenzierung von Neuroblasten bei *Leptodora kindti* Focke 1844 (Cladocera, Crustacea). Humboldt-University Berlin, Diploma thesis, pp 60
- Goodrich AL (1939) The origin and fate of the entoderm elements in the embryogeny of *Porcellio laevis* Latr. and *Armadillidium nasatum* B.L. (Isopoda). *J Morph* 64:401–429
- Gruner HE (1954) Über das Coxalglied der Peripoden der Isopoden. *Zool Anz* 152:312–317
- Gruner H-E (1965) *Krebstiere oder Crustacea, V. Isopoda (erster Teil)*. In: Dahl F (ed) *Die Tierwelt Deutschlands*, 51. Teil. Gustav Fischer, Jena, p 149
- Gruner H-E (1966) *Krebstiere oder Crustacea, V. Isopoda (zweiter Teil)*. In: Dahl F (ed) *Die Tierwelt Deutschlands*, 53. Teil. Gustav Fischer, Jena, p 230
- Gruner H-E (1993) Klasse Crustacea. In: Gruner H-E (ed) *Lehrbuch der speziellen Zoologie*. Gustav Fischer, Jena, pp 448–1009, Band 1: Wirbellose Tiere, 4. Teil: Arthropoda (ohne Insecta)
- Hahnenkamp L (1974) *Die Bildung und Differenzierung des Keimstreifs der Asseln (Isopoda) und anderer höherer Krebse. Eine vergleichend-embryologische Studie*. Berlin, Freie Universität. Hausarbeit für die erste (wissenschaftliche) Staatsprüfung, pp 180
- Hames CAC, Hopkin SP (1989) The structure and function of the digestive system of terrestrial isopods. *J Zool* 217:599–627
- Hansen HJ (1925) *Studies on Arthropoda II. On the comparative morphology of the appendages in the Arthropoda*. A. Crustacea. Gyldendalske Boghandel, Copenhagen, p 157
- Hartenstein V (1993) *Atlas of Drosophila development*. Cold Spring Harbor Laboratory Press, Cold Spring Harbor, p 57
- Havemann J, Müller U, Berger J, Schwarz H, Gerberding M, Moussian B (2008) Cuticle differentiation in the embryo of the amphipod crustacean *Parhyale hawaiensis*. *Cell Tissue Res* 332:359–370
- Hejnol A, Scholtz G (2004) Clonal analysis of *Distal-less* and *engrailed* expression patterns during early morphogenesis of uniramous and biramous crustacean limbs. *Dev Genes Evol* 214:473–485
- Hejnol A, Schnabel R, Scholtz G (2006) A 4D-microscopic analysis of the germ band in the isopod crustacean *Porcellio scaber* (Peracarida, Malacostraca)—developmental and phylogenetic implications. *Dev Genes Evol* 216:755–767
- Hickman VV (1937) The embryology of the syncarid crustacean, *Anaspides tasmaniae*. *Paps Proc Roy Soc Tasmania* 1–35

- Hoesle B (1981) Morphologie und Funktion des Wasserleitungssystems der terrestrischen Isopoden (Crustacea, Isopoda, Oniscoidea). *Zoomorphology* 98:135–167
- Hoesle B (1983) Structures and development of the lungs in Tylidae (Crustacea, Isopoda, Oniscoidea). *Zool Jb Anat* 109:487–501
- Hoesle B, Janssen HH (1989) Morphological and physiological studies on the marsupium in terrestrial isopods. *Ital J Zool* 4:153–173
- Holdich DM (1973) The midgut/hindgut controversy in isopods. *Crustaceana* 24:211–214
- Jaume D (2001) A new atlantasellid isopod (Asellota: Aselloidea) from the flooded coastal karst of the Dominican Republic (Hispaniola): evidence for an exopod on a thoracic limb and biogeographical implications. *J Zool* 255:221–233
- Kajishima T (1952) Experimental studies on the embryonic development of the isopod crustacean, *Megaligia exotica* Roux. *Annat Zool Jap* 25:172–181
- Knopf F, Koenemann S, Schram FR, Wolff C (2006) The urosome of the pan- and Peracarida. *Cont Biol* 75:1–21
- Kreissl S, Uber A, Harzsch S (2008) Muscle precursor cells in the developing limbs of two isopods (Crustacea, Peracarida): an immunohistochemical study using a novel monoclonal antibody against myosin heavy chain. *Dev Genes Evol* 218:253–265
- Lauterbach KE (1975) Über die Herkunft der Malacostraca (Crustacea). *Zool Anz* 194:165–179
- Liu Y, Maas A, Waloszek D (2009) Early development of the anterior body region of the grey widow spider *Latrodectus geometricus* Koch, 1841 (Theridiidae, Araneae). *Arthr Struct Dev* 38:401–416
- Manton SM (1928) On the embryology of a mysid crustacean, *Hemimysis lamornae*. *Phil Trans Roy Soc London* 216:363–463
- McMurrich JP (1895) Embryology of the isopod Crustacea. *J Morph* 11:63–154
- Morgan TH (1891) A contribution to the embryology and phylogeny of the pycnogonids. *Stud Biol Lab J Hopkins Univ* 5:1–76
- Nair SG (1956) On the embryology of the isopod *Irona*. *J Dev Exp Morph* 4:1–33
- Nusbaum J (1891) Beiträge zur Embryologie der Isopoden. *Zool Anz* 11:42–49
- Powell CVL, Halcrow K (1985) Formation of the epicuticle in a marine isopod, *Idotea baltica* (Pallas). *J Crust Biol* 5:439–448
- Richter S, Scholtz G (2001) Phylogenetic analysis of the Malacostraca (Crustacea). *J Zool Syst Evol Res* 39:113–136
- Samter M (1900) Studien zur Entwicklungsgeschichte der *Leptodora hyalina* Lillj. *Z Wiss Zool* 68:169–260
- Schmidt C, Wägele JW (2001) Morphology and evolution of respiratory structures in the pleopod exopodites of terrestrial Isopoda (Crustacea, Isopoda, Oniscoidea). *Act Zool* 82:315–330
- Scholl G (1963) Embryologische Untersuchungen an Tanaidaceen (*Heterotanais oerstedii* Kröyer). *Zool Jb Anat* 80:500–554
- Scholtz G (1995) Expression of the *engrailed* gene reveals nine putative segment-anlagen in the embryonic pleon of the freshwater crayfish *Cherax destructor* (Crustacea, Malacostraca, Decapoda). *Biol Bull* 188:157–165
- Scholtz G (1997) Cleavage, germ band formation and head segmentation: the ground pattern of the Euarthropoda. In: Fortey RA, Thomas RH (eds) *Arthropod relationships*, vol 24. Chapman & Hall, London, pp 317–332
- Scholtz G, Dohle W (1996) Cell lineage and cell fate in crustacean embryos—a comparative approach. *Int J Dev Biol* 40:211–220
- Scholtz G, Wolff C (2002) Cleavage, gastrulation, and germ disc formation in the amphipod *Orchestia cavimana* (Crustacea, Malacostraca, Peracarida). *Cont Biol* 71:9–28
- Schram FR (1986) *Crustacea*. Oxford Press, New York, p 606
- Shiino SM (1942) Studies on the embryology of *Squilla oratoria* de Haan. *Mem Coll Sci Kyoto Imp Univ Series B* 17:77–174
- Snodgrass RE (1952) *A textbook of arthropod anatomy*. Comstock, Ithaca, p 363
- Strömberg J-O (1965) On the embryology of the isopod *Idotea*. *Ark Zool* 17:421–467
- Strömberg J-O (1967) Segmentation and organogenesis in *Limnoria lignorum* (Rathke) (Isopoda). *Ark Zool* 20:91–139
- Strömberg J-O (1971) Contribution to the embryology of bopyrid isopods; with special reference to *Bopyroides*, *Hemiarthrus* and *Pseudione* (Isopoda, Epicaridea). *Sarsia* 47:1–47
- Strömberg J-O (1972) *Cyathura polita* (Crustacea, Isopoda), some embryological notes. *Bull Mar Sci* 22:463–482
- Strus J, Drobne D, Licar P (1995) Comparative anatomy and functional aspects of the digestive system in amphibious and terrestrial isopods (Isopoda: Oniscoidea). In: Alikhan MA (ed) *Crustacean Issues 9; terrestrial isopod biology*. A.A. Balkema, Rotterdam, pp 15–23
- Strus J, Klepal W, Repina J, Tusek-Znidaric M, Milatovic M, Pipan Z (2008) Ultrastructure of the digestive system and the fate of midgut during embryonic development in *Porcellio scaber* (Crustacea: Isopoda). *Arthr Struct Dev* 37:287–98
- Takashima S, Mkrtychyan M, Younossi-Hartenstein A, Merriam JR, Hartenstein V (2008) The behaviour of *Drosophila* adult hindgut stem cells is controlled by Wnt and Hh signalling. *Nature* 454:651–656
- Thiele J (1905) Betrachtungen über die Phylogenie der Crustaceenbeine. *Z Wiss Zool* 82:445–471
- Tomescu N, Craciun C (1987) Postembryonic ontogenetic development in *Porcellio scaber* (Crustacea, Isopoda). *Pedobiologia* 30:345–350
- Ungerer P, Wolff C (2005) External morphology of limb development in the amphipod *Orchestia cavimana* (Crustacea, Malacostraca, Peracarida). *Zoomorphology* 124:89–99
- Wägele JW (1992) Isopoda. In: Harrison FW, Humes AG (eds) *Microscopic anatomy of invertebrates, Crustacea*, vol 9. Wiley-Liss, New York, pp 529–617
- Waloszek D (1999) On the Cambrian diversity of Crustacea. Crustaceans and the biodiversity crises. *Proceedings of the 4th International Crustacean Congress*. Brill, Amsterdam, pp 3–27
- Waloszek D (2003) Cambrian ‘Orsten’-type arthropods and the phylogeny of Crustacea. The new panorama of animal evolution. *Proceedings of the 18th International Congress of Zoology*. Pensoft, Athens, pp 71–88
- Weygoldt P (1958) Die Embryonalentwicklung des Amphipoden *Gammarus pulex pulex* (L.). *Zool Jb Anat* 77:51–110
- Whittington PM, Leach D, Sandeman R (1993) Evolutionary change in neural development within the arthropods: axogenesis in the embryo of two crustaceans. *Development* 118:449–461
- Wilson GDF (2009) The phylogenetic position of the Isopoda in the Peracarida (Crustacea: Malacostraca). *Arthr Syst Phyl* 67:159–198
- Wolff C, Scholtz G (2008) The clonal composition of biramous and uniramous arthropod limbs. *Proc R Soc B* 275:1023–1028
- Zidar P, Van Gestel CAM, Strus J (2009) Single and joint effects of Zn and Cd on *Porcellio scaber* (Crustacea, Isopoda) exposed to artificially contaminated food. *Ecotoxicol Environ Saf* 72:2075–2082